

THE ENTEROHEMORRHAGIC *ESCHERICHIA COLI* EFFECTOR PROTEIN
NLEF BINDS MAMMALIAN HOST PROTEINS

By

Rachel L. Olsen

Submitted to the graduate degree program in Microbiology, Molecular Genetics and Immunology and the Graduate Faculty of the University of Kansas in partial fulfillment of the requirements for the degree of Master of Arts.

Committee:

Thomas Yankee, Pharm. D., Ph.D, Chairperson

Philip R. Hardwidge, Ph.D.

Mohammad Mir, Ph.D

Date Defended: 11/15/2012

The Thesis Committee for Rachel L. Olsen
certifies that this is the approved version of the following thesis:

THE ENTEROHEMORRHAGIC *ESCHERICHIA COLI* EFFECTOR PROTEIN
NLEF BINDS MAMMALIAN HOST PROTEINS

Committee:

Thomas Yankee, Pharm. D., Ph.D, Chairperson

Date Approved: 11/21/12

Abstract

The extracellular human pathogens enterohemorrhagic and enteropathogenic *Escherichia coli* (EHEC and EPEC) and the related mouse pathogen *Citrobacter rodentium* inject type III secretion system (T3SS) effector proteins to promote their replication, survival and transmission. The mechanisms of action and the host targets of T3SS effectors are under active investigation because of their importance to bacterial virulence. The non-locus of enterocyte effacement (LEE)-encoded protein F, NleF, contributes to *E. coli* and *Citrobacter* colonization of animals through an unclear mechanism. Here we sought to characterize the host binding partners of NleF. Using a yeast two-hybrid screen, we identified a set of mammalian proteins as NleF-binding partners including Tmp21, a type-I integral membrane protein and COPI-vesicle receptor involved in trans-Golgi network function. We confirmed this interaction using bacterial two-hybrid, immunoprecipitation and bimolecular fluorescence complementation (BiFC). To consider the effects of NleF on protein trafficking, we expressed a temperature-sensitive vesicular stomatitis virus glycoprotein (VSVG) with temperature dependent localization and monitored protein trafficking. We determined that NleF does not block, but rather slows the intracellular trafficking of VSVG from endoplasmic reticulum to Golgi.

Acknowledgments

I am first and foremost grateful to my research mentor Dr. Philip Hardwidge for his guidance and support of my research during my time in his lab. His continued patience and encouragement were an integral part of completing this task. I thank Dr. Thomas Yankee and Dr. Mohammad Mir, as well, for serving on my thesis committee and their willingness to support me in the completion of this achievement.

I also want to thank many other people who played a role in this journey including previous and current members of the Hardwidge lab. I especially thank Dr. Dilyara Cheranova for beginning the experiments that initiated this path of study. I want to give special mention to Dr. Leigh Ann Feuerbacher and Dr. Xiaogang Wang for their advice in both experimental and writing aspects and their friendship. Dr. Flavia Costa has also been an invaluable peer and friend providing both exceptional advice and a patient ear.

Finally, I want to acknowledge my husband Nathaniel for his love and steadfastness throughout the frustrations and his help in caring for our beautiful daughter Temperance Rós. I wish to express my gratitude to my father Denis Grau for our many scientific conversations over the years and his constant encouragement and to my brother Matthew Grau for the necessary comic relief. I also want thank to both my Father and Mother-in-Law Stan and Pat Olsen and my Brother and Sister-in-Law Brent and Nisse Bjornsen for their continued reassurance and prayers. I appreciate all the support from the rest of my family as well. Lastly, I want to thank my best friend Carrie Clark(Spiers), who has been there for me for most of our lives and has played a special role in my life and studies.

Table of Contents

DATE DEFENDED	I
DATE APPROVED	II
ABSTRACT	III
ACKNOWLEDGMENTS	IV
TABLE OF CONTENTS	V
LIST OF FIGURES	VI
LIST OF TABLES	IX
ABBREVIATIONS	X
CHAPTER 1 INTRODUCTION	1
1.1 SCOPE OF THIS STUDY	2
1.2 FOODBORNE ILLNESS AND DISEASES CAUSED BY <i>ESCHERICHIA COLI</i>	3
1.2.a <i>Foodborne Illness</i>	3
1.2.b <i>Bacterial Gastroenteritis</i>	4
1.2.c <i>Hemorrhagic Colitis and Hemolytic Uremic Syndrome</i>	4
1.3 ATTACHING AND EFFACING <i>ESCHERICHIA COLI</i>	5
1.3.a <i>Enteropathogenic E. coli</i>	6
1.3.b <i>Enterohemorrhagic E. coli</i>	7
1.3.c <i>Citrobacter rodentium</i>	8
1.4 VIRULENCE FACTORS AND TRAITS OF ENTEROHEMORRHAGIC <i>ESCHERICHIA COLI</i>	9
1.4.a <i>Adhesion, Type III Secretion System, and lesion formation</i>	9
1.4.b <i>Regulation</i>	11
1.4.c <i>Toxins</i>	12
1.4.d <i>NleF</i>	13
1.5 THE MAMMALIAN PROTEIN SECRETORY PATHWAY: PROCESSES, COMPONENTS, AND SUBVERSION.....	14
1.5.a <i>From protein synthesis to secretion and pathogen manipulation</i>	14
1.5.b <i>The p24 protein family: structure and function</i>	16
1.5.c <i>Tmp21</i>	17
CHAPTER 2 MATERIALS AND METHODS.....	18
2.1 BACTERIAL STRAINS, CELL CULTURE, AND INFECTION	19
2.2 PROTEIN PURIFICATION	19
2.3 PROTEIN PULL DOWN ASSAY.....	24
2.4 YEAST TWO-HYBRID SCREEN.	25
2.5 BACTERIAL TWO-HYBRID ASSAY.	27
2.6 IMMUNOFLUORESCENT DETECTION OF CO-LOCALIZATION.....	29
2.7 BIMOLECULAR FLUORESCENCE COMPLEMENTATION PLASMID CONSTRUCTION AND ASSAY.	30
2.8 IMMUNOBLOTTING.....	32
2.9 VSVG PROTEIN TRAFFICKING ASSAY.	33
2.10 APOPTOSIS ASSAY.	35

CHAPTER 3 RESULTS.....	36
3.1 YEAST-TWO HYBRID SCREEN AND OF NLEF MAMMALIAN BINDING PARTNERS.....	37
3.2 BACTERIAL-TWO HYBRID VERIFICATION OF NLEF MAMMALIAN BINDING PARTNERS.	37
3.3 CO-IMMUNOPRECIPITATION OF NLEF AND TMP21.	40
3.4 NLEF AND TMP21 CO-LOCALIZE.	40
3.5 BIMOLECULAR FLUORESCENT COMPLEMENTATION ANALYSIS SUPPORTS INTERACTION OF NLEF AND TMP21.	43
3.6 NLEF ALTERS VSVG-GFP TRAFFICKING.	46
3.7 NLEF DOES NOT INDUCE APOPTOSIS IN MAMALIAN COLORECTAL CANCER CELLS.....	51
CHAPTER 4 DISCUSSION	53
CHAPTER 5 REFERENCES.....	61

List of Figures

FIGURE 1. BACTERIAL TWO-HYBRID ASSAY SCHEMATIC.	28
FIGURE 2. BIMOLECULAR FLUORESCENCE COMPLEMENTATION ASSAY SCHEMATIC.	31
FIGURE 3. VSVG TRAFFICKING SCHEMATIC.	34
FIGURE 4: MEASUREMENT OF NLEF BINDING TO TMP21 WITH THE β-GALACTOSIDASE ASSAY.	38
FIGURE 5: TMP21 IS IMMUNOPRECIPITATED WITH NLEF	41
FIGURE 7: NLEF AND TMP21 CO-LOCALIZE IN HELA CELLS.	42
FIGURE 7: FULL LENGTH NLEF AND TMP21 EXPRESSION AND FLUORESCENCE QUANTIFICATION...	44
FIGURE 8: NLEF AND TMP21 TRUNCATION EXPRESSION AND INTERACTION VERIFICATION.	45
FIGURE 9: VERIFICATION OF HA CONTROL STAINING IN HELA CELLS.	47
FIGURE 11: NLEF ALTERS VSVF-GFP TRAFFICKING IN REFERENCE TO THE ENDOPLASMIC RETICULUM WHEN DELIVERED BY TRANSFECTION.	48
FIGURE 11: NLEF ALTERS VSVF-GFP TRAFFICKING IN REFERENCE TO THE GOLGI WHEN DELIVERED BY TRANSFECTION.	49
FIGURE 12: NLEF ALTERS VSVF-GFP TRAFFICKING WHEN DELIVERED BY INFECTION.	50
FIGURE 13: NLEF DOES NOT INDUCE APOPTOSIS IN COLORECTAL ADENOCARCINOMA CELLS.	52
FIGURE 14: EHEC EFFECTOR PROTEIN ALTERATION OF TRAFFICKING.	59

List of Tables

TABLE 1. STRAINS USED IN THIS STUDY.....	21
TABLE 2. PLASMIDS USED IN THIS STUDY.	22
TABLE 3. OLIGONUCLEOTIDES USED IN THIS STUDY.....	23
TABLE 4. BACTERIAL TWO-HYBRID ANALYSIS OF POTENTIAL PROTEIN-PROTEIN INTERACTION BETWEEN NLEF AND IDENTIFIED MAMMALIAN PROTEINS.....	39

Abbreviations

A/E: Attaching and effacing

BiFC: Bimolecular fluorescence complementation

BFP: Bundle forming pilus

C. rodentium: *Citrobacter rodentium*

Cb: Carbenicillin

CDC: Centers for Disease Control and Prevention

CNS: Central Nervous System

DMEM: Dulbecco's modified Eagle's medium

EAF: *E. coli* adherence factor

Esp: *E. coli* secreted protein

EHEC: Enterohemorrhagic *E. coli*

EPEC: Enteropathogenic *E. coli*

ER: Endoplasmic reticulum

ERES: Endoplasmic reticulum exit sites

ETEC: Enterotoxigenic *E. coli*

FBS: Fetal bovine serum

Gb3: Glycolipid globotriaosylceramide

GI: Gastrointestinal

IC: Intermediate compartment

HC: Hemorrhagic colitis

HUS: Hemolytic uremic syndrome

LB: Luria-Bertani broth

LEE: Locus of enterocyte effacement

Ler: LEE encoded regulator

LPS: Lipopolysaccharide

Nle: Non-LEE-encoded

PAI: Pathogenicity Island

PCR: Polymerase chain reaction

PM: Plasma membrane

RTX: Repeats in toxin

SRP: Signal recognition particle

STE: Sodium Chloride-Tris-EDTA Buffer

STEC: Shiga Toxin producing *E. coli*

Stx: Shiga toxin

T3SS: Type III secretion system

TD: Transmembrane domain

TGN: Trans Golgi Network

Tir: Translocated intimin receptor

TMED10: Transmembrane emp24-like trafficking protein 10

PKC δ : Protein kinase C delta

Chapter 1
INTRODUCTION

1.1 Scope of this study

Enterohemorrhagic *Escherichia coli* (EHEC) is one of the leading causes of foodborne illness globally. Strains linked to human disease survive within other species harmlessly. Only upon discharge into the environment within manure, as crop fertilizer or run off, or via contamination of food sources, such as improperly processed beef, do these strains find their way into humans. Infections connected to EHEC represent a significant financial burden to both the beef and health care industries. The beef industry has experienced losses of millions of pounds of ground beef within a single outbreak and health care institutions suffer the expense of treatment of EHEC, which represents the 5th most common cause of foodborne infection hospitalization in the United States [1]. With no prophylaxis or specific treatment available for EHEC infections, understanding the many ways employed by EHEC, and other similar *E. coli* pathotypes, such as *Enteropathogenic E. coli*, to productively infect its host is essential to prevention of future outbreaks and development of improved therapies.

The capacity of *E. coli* to cause infection depends on its numerous virulence factors, the best-understood of which include those involved in bacterial adherence to host cells (Tir and Intimin) and the Type III Secretion System injectisome. A substantial number of virulence factors known as translocated effector proteins also exist, which the bacterium introduces into the host cell by injecting them through the injectisome effectively delivering them directly into the host cells cytoplasm. Effectors with known function have been found to target host proteins and pathways in order to hijack or subvert function and permit successful infection. However, many of the effectors identified have as yet

unknown function. NleF belongs to the latter group of effectors, but it has demonstrated to play a role in colonization and virulence [2]. As such, delineation of NleF specific host targets and the mechanisms by which it enables infection would provide additional therapeutic targets. The goal of this study was to verify mammalian Tmp21 as an NleF host target and to dissect the mechanism by which this interaction plays a role in *E. coli* colonization and virulence. Our study provides the first evidence of NleF alteration in protein trafficking of the secretory pathway via interaction with the COPI binding p24 family member Tmp21.

1.2 Foodborne illness and diseases caused by *Escherichia coli*

Escherichia coli is a major etiological agent of foodborne disease. Gastroenteritis is commonly found with *E. coli* infections and progression to more serious illnesses, such as Hemorrhagic Colitis and Hemolytic Uremic Syndrome, increases when Shiga Toxin-Producing *E. coli* (STEC) are the source.

1.2.a Foodborne Illness

Foodborne illness is a continuing problem in the developed world. The typical source of illness originates from improper storage and handling or contamination of food products prior to use [3]. The Centers for Disease Control and Prevention (CDC) 2011 estimates indicate 1 in every 6 Americans (48 million) become ill as a result of contaminated food sources. Health costs are high for treatment of those that are hospitalized (128,000) and death occurs in less than 1 % (3,000). While the hospitalizations and deaths seem to comprise a small percentage of cases, these are representative of only those reported.

Illnesses are categorized into two groups: known foodborne pathogens or unspecified agents. Roughly 20 % of all reported cases originate from infection by one of 31 known pathogens and 18 % overall are linked to the major 7 which include Salmonella, Campylobacter, and *E. coli* O157:H7. At 2 %, *E. coli* ranks in the top 5 of these pathogens for resulting hospitalizations [4].

1.2.b Bacterial Gastroenteritis

Bacterial gastroenteritis is an inflammation of the stomach and intestines resulting from infection by a pathogenic strain of bacteria [5-7]. The range of symptoms is variable dependent on the source organism [8]. However, diarrhea is found in all forms of foodborne illness and additional symptoms can include abdominal cramping and pain, reduced appetite, nausea and vomiting [5-11]. Treatment begins after identification of the infecting organism and mainly involves rest, hydration maintenance, and control of nausea and vomiting [8]. Source identification is crucial as it is necessary to avoid antibiotic treatment in the case of infections by STEC to prevent more severe symptoms and outcomes [12-16].

1.2.c Hemorrhagic Colitis and Hemolytic Uremic Syndrome

A specific form of gastroenteritis, Hemorrhagic Colitis (HC), is caused by infection of the large intestines and toxin production by STEC. *E. coli* O157:H7 is the most common source of HC causing infection in the US and sometimes results in bloody diarrhea in the young and elderly populations due to toxin damage of the intestinal epithelium [17-20]. As with general gastroenteritis, abdominal cramping coincides with production of watery diarrhea. Diarrhea may become bloody within 1-3 days [21]. Resolution of

diarrhea typically occurs within the following week [9-11]. Importantly, patients are often afebrile, a hallmark of infection with STEC [22]. Approximately 10 % of those who progress to HC will subsequently develop a severe condition known as Hemolytic Uremic Syndrome (HUS) in the second week of infection (7-10 days) preceded by increased fever [9, 11, 23-26]. *E. coli* is the most common cause of documented HUS (90 %), which is characterized by hemolytic anemia and thrombocytopenia resulting in fatigue and lightheadedness due to red blood cell lysis, uremia, and oliguria [9, 27]. Further complications of the CNS can develop with nerve and brain damage leading to seizures or strokes [28]. There is no targeted treatment available so care is focused on providing ample hydration to counter dehydration as a consequence of the severe and prolonged diarrhea [29]. Many recover fully but, despite treatment, some develop chronic kidney disease and mortality occurs in 5-10 % of patients [21].

1.3 Attaching and effacing *Escherichia coli*

E. coli are gram-negative, rod shaped enteric bacteria with numerous species residing in the human gastrointestinal tract [20]. The commensal strains of the GI microbiota are innocuous and provide host health benefits, such as protection against infection and nutrient acquisition [30]. However, certain groups of *E. coli strains* have evolved into pathogens now linked to human diarrheal diseases through assimilation of virulence genes via transfer of mobile genetic elements [31, 32]. Most infections are a product of ingestion of contaminated or improperly handled food sources, though some may be transmitted by direct contact with infected individuals and animals [3, 23, 33]. There are approximately 9 pathogenic groups recognized, which are organized based on their

virulence traits or factors. These groups include: enteropathogenic *E. coli* (EPEC), enterohemorrhagic *E. coli* (EHEC), enterotoxigenic *E. coli* (ETEC), enteroinvasive *E. coli* (EIEC), enteroaggregative *E. coli* (EAEC), and diffusely adherent *E. coli* (DAEC) [26]. The attaching and effacing (A/E) strains of *E. coli* are extracellular pathogens and are characterized by their capacity to destroy the intestinal microvilli (brush border) and induce formation of a pedestal through manipulation of the host cell cytoskeleton [26, 34-36].

1.3.a Enteropathogenic *E. coli*

EPEC was the first described pathotype of *E. coli* in 1945 after an infant diarrheal outbreak in the UK. The occurrence of similar outbreaks has diminished in recent years and mortality rates have fallen significantly from the 25-50 % noted prior to improved treatments [37, 38]. Regardless, EPEC continues as a significant source of diarrheal outbreaks in the developing world in children under 2 years of age [37, 39]. Onset of the main symptom, diarrhea, occurs within 4 hours of infection and advances to addition of vomiting and low-grade fevers in some cases [38]. Correction of fluid loss must occur quickly to avoid dehydration. Duration of infant diarrhea is protracted and can persist from 22 days to 120 days in severe cases. The primary route of infection is oral, however this pathotype is linked with considerable transmission by contact with infected individuals, rather than by ingestion of contaminated food, as evidenced by the sporadic nature of foodborne outbreaks [38]. Diagnosis is accomplished through tissue culture infection analysis to assess whether characteristic pathology associated with attaching and effacing pathotypes is observed. Positive isolates cause typical intimate intestinal

epithelial attachment, microvilli destruction, and cytoskeletal polymerization producing pedestal protrusions from the epithelial surface. PCR detection of the locus of enterocyte effacement (LEE) pathogenicity island genes responsible for these processes is also employed, but is not sufficient as many of these genes are homologous to genes found in other A/E pathotypes, including EHEC and *Citrobacter rodentium*. Verification of shiga toxin absence is necessary for ultimate identification of non-toxigenic EPEC.

1.3.b Enterohemorrhagic *E. coli*

The EHEC pathotype is foremost associated with production of Shiga toxin (Stx), which classifies them as STEC. The number of STEC serotypes recognized varies between sources, but reaches numbers upwards of 200 including strains not linked to illness. Strain O157:H7 is responsible for ~75 % of worldwide *E. coli* infections and is the model for the EHEC subset, which includes only strains proven to cause severe disease. Other strains in this subset have caused major outbreaks including the O104:H4 strain 2011 outbreak in Germany. However, though a producer of Stx this strain may not be correctly classified as EHEC based on high genetic homology with an EAEC strain [4, 38].

The major reservoir for EHEC is the bovine intestinal tract with high colonization of the rectal-anal junction found in super-shedders, which are responsible for >90 % of EHEC spread [13, 40, 41]. Foodborne transmission through ingestion of foods contaminated with infectious manure is the typical route of infection. EHEC, like EPEC, possess the

locus for enterocyte effacement pathogenicity island (LEE), encoding more than 20 proteins including factors involved in virulence mechanisms, such as attachment to host epithelium (intimin, Tir) and delivery of virulence factors into host cells (T3SS) [42]. O157:H7 do not ferment sorbitol, unlike commensal strains, and this can be used for detection by culturing on sorbitol MacConkey agar and screening for non-fermenting strains [11]. Serotyping of the O and Flagellar antigens, PCR, and Stx detection methods are also employed for identification. The infective dose is as low as 10 organisms, while other strains are thought to require higher doses. Symptoms appear as early as 3 days post infection, but can sometimes require longer incubations extending 9 days post infection. Infection may be asymptomatic in some hosts, however diarrhea presents in the majority of infected individuals. Additionally, a small percentage of the infected develop acute Hemorrhagic Colitis followed by severe Hemolytic Uremic Syndrome in serious cases. The populations most susceptible to EHEC infection are the young and elderly and the immune-compromised [38]

1.3.c *Citrobacter rodentium*

Citrobacter rodentium targets mice as a natural host and infection causes high mortality transmissible murine colonic hyperplasia in some mouse strains, detectable within 5-14 days post infection [43]. Infection is not limited to the intestines and the pathogen may sometimes cause opportunistic effects in other organs and tissues. Colonization of the caecum is observed within a few hours of high dose infection (10^8 - 10^9) progressing to the distal colon within a few days and clearance in 21-28 days [44]. Due to the ability to easily modify the strain genetically, it is employed in mice as an *in vivo* model for A/E pathogens to consider infection from the perspective of both the pathogen and of the

host immune response [43, 45-50]. More importantly, the strain is ideal model for EPEC and EHEC as the A/E genes encoded on the conserved LEE pathogenicity island of *C. rodentium* are highly homologous with the EPEC and EHEC genes [51].

1.4 Virulence factors and traits of Enterohemorrhagic Escherichia coli

E. coli possess a sizeable collection of virulence factors/traits and the numerous strategies they employ to permit successful infection and survival in the host have not been fully elucidated. This is particularly true in the case of the dozens of identified effector proteins with currently undetermined roles. Classification of those effectors on the basis of known functions and properties can be very broad and includes, but is not limited to, categories encompassing cell surface adhesion/lesion formation, effector delivery/translocation (T3SS), gene regulation, and toxins. Account of some representative factors in these categories, their attributes, and involvement in pathogenesis follows.

1.4.a Adhesion, Type III Secretion System, and lesion formation

Colonization for A/E pathogens is dependent on adhesion to the surface of intestinal mucosae to overcome mechanical host defense barriers. As the bacterium is propelled through the host by peritrichous flagella, environmental cues, such as temperature and bacterial signaling, prompt *E. coli* to present adhesins in the form of surface fimbriae. These fimbriae are threadlike protein polymers, which come into contact with the intestinal epithelium [52]. Processes involved in A/E lesion formation follow and are similar for EPEC and EHEC, though they do not share all of the same adhesin genes. The EAF (*E. coli* adherence factor) plasmid is carried by some EPEC strains, but not

EHEC, and encodes a type IV BFP (Bundle forming pilus) [53]. The pilus is required to cause diarrhea, yet its role is more significant in the late infection stage for EPEC aggregate formation than in initial interaction between the bacterium and host [54-59]. EHEC instead encode two fimbrial operons analogous to the LPF (long polar fimbriae) of salmonella, *lpf* and *lpfA*, which are also not present in EPEC [60].

Contact with the host cell provides the stimulus to induce synthesis of Type III Secretion System (T3SS) components. The T3SS is a molecular syringe, structurally similar to flagella, found in many gram-negative bacteria and all of the A/E strains [36, 61]. This secretion apparatus delivers cytoplasmic bacterial effector proteins directly into the host cells [62]. The basal structure of the injectisome consists of two rings creating pores in the interior and exterior bacterial membrane [63]. The rings are comprised of over 20 identified proteins and serve as the foundation for the flexible syringe filament, composed of the protein EspA, which extends as a hollow sheath from the bacterium to come in direct contact with the host cell [64]. Contact facilitates formation of a pore in the host membrane through the action of other translocated proteins including EspB, and permits translocation of bacterial effector proteins into the host cell [65, 66]. Tir is next delivered through the EspA filament whereupon it embeds into the host membrane and acts as a receptor to the Intimin adhesin expressed on the bacterial surface [67]. Interaction between Tir and Intimin prompts a shortening of the EspA filament, ultimately drawing the *E. coli* into intimate contact with the host cell [68, 69]. Signal transduction pathways are correspondingly activated leading to host cytoskeleton rearrangement and brush border destruction. The cytoskeletal alterations bring about

formation of a pedestal-like protrusion from the host cell surface, on which the bacterium rests. Delivery of effector proteins continues via translocation through the T3SS syringe. Of note, EspB and EspD translocated proteins both function in and are required for subsequent A/E lesion formation [70-72].

1.4.b Regulation

Expression of all virulence-associated genes in *E. coli* is not constitutive, making regulation of gene expression crucial to proper production and coordination of virulence factors. The LEE encoded regulator (*Ler/orf1*), is a DNA binding protein homologous to members of the histone-like H-NS family of proteins known for their ability to repress gene expression [57, 58, 73, 74]. *Ler* is responsible for regulation of all genes central to formation of A/E lesions [74, 75]. In the absence of activating signals, H-NS is bound to the promoter regions of the LEE operons and silences or blocks transcription of virulence genes. The bacterium receives environmental cues that lead to induction of *Ler* transcription. Once sufficient levels of *Ler* are available it displaces H-NS, thus freeing the promoters for ribosome binding and protein transcription [75-79]. Direct regulation of *Ler* is maintained by two other LEE encoded proteins of opposing function: *GrIA* and *GrIR*. *GrIA* is a positive regulator of *Ler* transcription and is unbound during the stationary phase when induction of LEE encoded genes is necessary [2, 80, 81]. During the growth phase *GrIR* levels rise when it acts as a negative regulator of *Ler* transcription by binding to *GrIA* and preventing upregulation of LEE expression [81-83].

1.4.c Toxins

Hemolysin is an example of an incompletely characterized, but well conserved, toxin found in a population of enterohemorrhagic *E. coli* serotypes [84]. The EHEC hemolysin is structurally similar to the prototypical RTX pore-forming toxins found in Gram-negative microorganisms and thought to increase iron availability through lysis of host red blood cells [85-87]. Stx is a notably more significant *E. coli* virulence factor, as shiga-like toxin production is a required characteristic of STEC *E. coli* pathotypes. *Shigella dysenteriae* produces the “true” shiga toxin, whereas *E. coli* strains produce one of the highly homologous bacteriophage encoded forms Stx-1 or Stx-2 [9, 88]. The Stx receptor in humans is the glycolipid globotriaosylceramide (Gb3), which is concentrated primarily on renal epithelium, but is also found in the CNS on both neurons and endothelial cells [88-90]. Both locations seem to correlate well with associated symptoms of HC and HUS (renal) and the accompanying neurological symptoms in severe cases [90]. The ability of Stx-2 to increase the Gb3 receptor in the CNS is an additional means of increasing the observed neurotoxicity in such cases [91]. Stx, an AB₅ toxin, is composed of a single A subunit and B subunit pentamer. The B pentamer binds Gb3 and the A subunit is internalized by pinocytosis where it is cleaved in two. The A subunit acts as N-glycosidase and, similarly to the ricin toxins function, host protein synthesis is halted as a result of cleavage of an adenine from the 28S RNA of the 60S ribosome [92-95]. Asymptomatic carriage and shedding of *E. coli* by reservoir species is therefore likely due to the absence of this receptor in those organisms [96].

1.4.d NleF

Non-LEE encoded effector F (NleF) was discovered in a proteomic screen of EHEC and *C. rodentium* targeted at identification of novel secreted proteins [2]. NleF is found more prevalently in *E. coli* outbreak lineages and those leading more frequently to human disease and development of HUS [97]. In the EHEC screen more than 20 proteins were distinguished as likely T3SS substrates [2]. Nles are not found in the locus of enterocyte effacement pathogenicity island, but rather are encoded in alternate PAIs and cryptic prophages. NleF is an 189 amino acid (21.4 kDa) protein encoded on the same PAI, O-island 71, as the previously characterized effector NleA. Sequencing demonstrated that homology to proteins of known function is absent, but sequence similarity was found with some uncharacterized proteins from *Yersinia pseudotuberculosis* (27 %, YPTB2540 and Ypsel_02001372) and *Shigella dysenteriae* (58 %, hypothetical protein SDY_P223). NleF amino acid identity of 100 % is shared between O157:H7 and other strains including EHEC Sakai and EPEC E2348/96, while an 85 % homology exists with the *Citrobacter rodentium* [98].

Much work has already been done to begin exploring the role played by NleF in infection. Initial recognition of NleF in the secreted proteins fraction of a super secreting sepL deletion mutant, combined with additional verification by comparative Western Blot of wild-type and T3SS mutant infection of host cells, identifies it as a secreted and T3SS-dependent translocated effector protein [2, 98, 99]. Validation through a TEM-1 based assay confirmed this translocation occurs. Previous studies determined amino acids 1-60 were sufficient to foster translocation and have also established NleF does not influence adherence to host cells or pedestal formation, nor was it found to disrupt

protein secretion or trafficking in the same manner as NleA [42, 98, 100]. Nonetheless, a contribution to colonization was evident in both competitive co-infection of mouse models with *C. rodentium* and gnotobiotic piglet infection with EHEC [98]. However, though all of this together maintains NleF is an effector protein playing a role in virulence, the host targets and specific function in pathogenesis have yet to be identified.

1.5 The mammalian protein secretory pathway: processes, components, and subversion.

Many points throughout the host protein trafficking/secretory pathways involving transit and processing have been targeted and exploited by bacterial pathogens, making this an area of great interest in the study of host-microbe interactions. *Salmonella*, for instance, alter recruitment of exocytic transport vesicles to *Salmonella*-containing vacuoles presumably to restrict antigen presentation and immune recognition [101]. *Legionella* spp. provide a nutrient source through recruitment of ER-derived vesicles to phagosomal membranes [102]. Interaction with host endocytic machinery by *S. enterica* effectors provides a modified phagosome-like vacuole wherein the survival and replication are protected from host defenses [103, 104]. Intracellular replication is manipulated by *Brucella abortus* use of the ER GTPase Sar1 [105]. Of particular interest in *E. coli* research, binding of Sec24 by NleA results in inhibition of COPII-dependent ER protein export [100].

1.5.a From protein synthesis to secretion and pathogen manipulation

The secretory pathway is an integral part of newly synthesized protein transit to either

target destinations within the cell or release from the cell through secretion. Proteins are generally synthesized in the cytoplasm and incorporated 20-30 amino acid hydrophobic signal sequences target them to the ER. Entry into the ER lumen may occur either co-translationally or post-translationally [106, 107]. Co-translational ER entry depends on recognition and binding of the N-terminal signal sequence hydrophobic core soon after translation commences. This is achieved by the signal recognition particle (SRP), which then targets the newly synthesized protein through binding to the SRP receptor embedded in the ER membrane and threads the peptide through the translocon co-translationally [108, 109]. For post-translational delivery this occurs after the complete peptide has been synthesized and released from the ribosome. Upon entry into the ER lumen, folding of the proteins begins and, as maturation proceeds, they are further altered co- and post-translationally through addition of modifications [110-113]. Modifications include formation of di-sulfide bridges, hydroxylation of prolines, and attachment to the peptide of molecules such as hydrophilic sugar moieties (N-linked glycosylation) [114]. Once properly folded, proteins continue on to their target locations. This involves packaging into COPII-coated transport vesicles and budding from the ER at exit sites (ERES) [110-113, 115-117]. Transport vesicles travel anterograde along microtubule networks to the Golgi [117]. In the Golgi additional post-translational modifications, such as sulfation and phosphorylation, may be incorporated into the mature proteins [118]. Moving in a cis-to-trans direction as cisternae are formed and travel to the trans side for release/dissolution, cargo proteins are gradually delivered to the Trans Golgi Network (TGN). There they are packaged into new vesicles targeted to their final post-Golgi destinations whether they be intracellular (lysosome/endosome) or

extracellular (PM or extracellular space) [119-122].

1.5.b The p24 protein family: structure and function.

Members of the p24 protein family are involved in early processes of the secretory pathway at the ER-Golgi interface [110-113]. The family is comprised of ~24 kDa type-I transmembrane proteins divided into four subfamilies: α - δ [123]. Shared structural characteristics of the family including an extracellular or luminal N-terminus, an N-terminal disulfide bridge containing a Golgi dynamics domain (GOLD), a single transmembrane domain, a coiled-coiled region and a 13-20 residue cytoplasmic tail [123-125]. Functionally, members are thought to act principally as bidirectional transport cargo receptors between the ER and Golgi. Other functions and localization to later compartments have also been proposed including a role in COPI vesicle biogenesis/anterograde transport, intracellular membrane organization and protein quality control [110-113, 123, 126-130]. COPI and COPII binding motifs are found in the cytoplasmic tail region and are highly conserved [125]. Family members occur primarily as monomers or as dimers through interaction between the coiled-coil regions and dimerization dependent movement of heteromeric complexes between secretory pathway subcompartments has been shown to occur continuously [123, 126, 131-143]. As plentiful constituents of transport vesicles and ER/Golgi membranes, p24 proteins are widely distributed in the cell and are therefore potential targets for sabotage by pathogens.

1.5.c Tmp21

Tmp21 (p23/TMED10), a 219 amino acid integral type I transmembrane protein, is an integral receptor for the COPI-vesicle coat and member of the p24 family of proteins [144]. The 12 amino acid cytoplasmic tail contains a conserved ER export FF motif near the Transmembrane Domain (TD) and a C-terminal KKLIE motif. Similarity of this motif to the KKXX ER retention and retrieval motif, also known to bind COPI, indicates Tmp21 as a probable COPI receptor [125, 135, 136, 143, 145-152]. KKLIE motif mutation results in loss of COPI binding, but no alteration in Tmp21 function. Localization is altered by KK to SS substitution resulting in abrogation of PM localization. Interaction with other p24 family members plays an additional role in localization as evidenced by variation in localization when Tmp21 is co-expressed with different members [141]. Functions are believed to include p24 family characteristic involvement in vesicle formation, cargo transport, and quality control [123, 126, 134-136, 153-156]. Localization is found mainly in the Vesicular Tubular Clusters, which comprise the intermediate compartment of from the ER to the Golgi [115, 157-159]. Trafficking of Tmp21 from the Intermediate Compartment (IC) to the Golgi is accomplished through use of microtubule-dependent vesicular tubular transport complexes [157, 160, 161]. However, additional studies have identified other Tmp21 localizations and more extensive functional roles, such as PM localized regulation of gamma secretase cleavage as a component of the presenilin complex and strong induction of apoptosis through association with PCK- δ in the LNCap prostate cancer cell line [162, 163].

Chapter 2
MATERIALS AND METHODS

2.1 Bacterial Strains, Cell Culture, and Infection

The bacterial strains and plasmids used in this study are described in Table 1 and Table 2. Oligonucleotide sequences for plasmids constructed for this study are in Table 3. HeLa cells were maintained in Dulbecco's modified Eagle's medium (DMEM) supplemented with 10 % fetal bovine serum (FBS). Cells were transfected using TransPass HeLa (England Biolabs). Bacteria were cultured in Luria-Bertani broth (LB) at 37 °C either overnight with shaking for all cultures except those intended for infection, which were incubated 18 h without shaking. Overnight LB cultures were diluted 1:10 into DMEM, followed by a further incubation for 3 h at 37 °C, 5 % CO₂. Cell culture media was replaced with DMEM prior to infection and bacteria were added at a multiplicity of infection of 25-50.

2.2 Protein Purification

NleF and Tmp21 were cloned into pFLAG-CTC and pET28a, respectively, and expressed in *E. coli* BL21(DE3). Bacterial cultures were grown to an OD600 of 0.2~0.5 and then induced with 1 mM IPTG for 2 h. Cells were pelleted for 10 minutes 5,000 g at 4 °C. NleF-FLAG pellets were resuspended in 10 ml 1X STE per 500 ml induced culture then lysed by sonication on ice 5X at 50 % for 30 seconds pulses with 30 second holds between each pulse. Lysate was transferred to 1.5 ml microcentrifuge tubes in 0.9 ml aliquots and kept on ice. To each tube 100 µl of detergent solubilization buffer, diluted 1:1 in 1X STE, was added and mixed by gentle inversion followed by a 1 hr incubation with inversion every 15 minutes. Lysates were pelleted for 15 minutes at 12,000 g in a 4 °C microcentrifuge. Supernatants were transferred to fresh 1.5 ml microcentrifuge tubes

and 100 μ l detergent neutralization buffer added to each followed by an addition 1 hour incubation with mixing by inversion every 15 minutes. Treated lysates were combined and to 200 μ l of ANTI-FLAG M2 resin for every 500 ml original culture then incubated at 4 °C overnight. Loaded resin was pelleted for 5 minutes 2,000 g at 4 °C the washed 5X with 1X STE. Protein was eluted with 500 μ L 0.1M glycine HCl pH 3.5 per elution by nutation at room temperature for 10 minutes for 3 consecutive elutions. Elutions were stored at -20 °C and concentrations verified by Bradford assay and SDS-PAGE gel.

Tmp21-His pellets were resuspended in 10 ml His-tag denaturing lysis buffer (100 mM NaCl, 20 mM Tris-Hcl pH 8.0, 6 M guanidine) per 100 ml induced culture then lysed by sonication on ice 5X at 50 % for 30 seconds pulses with 30 second holds between each pulse. Lysate was clarified by centrifugation for 15 minutes at 12,000 g in a 4 °C centrifuge. Supernatant was transferred to fresh pre-chilled tube containing 500 μ l per 250 ml original culture of pre-washed Ni-NTA agarose and incubated at 4 °C overnight. Agarose was pelleted for 5 minutes 2,000 g at 4 °C the washed 3X with His-Tag Denaturing Wash Buffer (100 mM NaCl, 20 mM Tris-Hcl pH 8.0, 6 M guanidine, 10 mM imidazole). Protein was eluted with 1.5 ml Elution Buffer 1 (100 mM NaCl, 20 mM Tris-Hcl pH 8.0, 6 M guanidine, 100 mM imidazole) by nutation at room temperature for 10 minutes. Agarose was pelleted for 5 minutes 2,000 g at 4 °C and the supernatant retained as elution 1. Two additional elutions for 10 minutes at room temperature using increasing concentration of imadazole (300 mM and 500 mM) were retained as elutions 2 and 3. Elutions were dialyzed overnight at 4 °C in sodium phosphate buffer (25 mM sodium phosphate pH 7.5, 1 mM DTT, 5 % glycerol) then stored at -80 °C. Elution concentrations were verified by Bradford assay and SDS-PAGE gel.

TABLE 1. STRAINS USED IN THIS STUDY.

Strain or plasmid	Genotype or description	Reference
Yeast strains		
AH109	<i>S. cerevisiae</i> MATa, <i>trp1-901, leu2-3, 112, ura3-52, his3-200, gal4D, gal80D, LYS2::GAL1_{UAS}-GAL1_{TATA}-HIS3, GAL2_{UAS}-GAL2_{TATA}-ADE2, URA3::MEL1_{UAS}-MEL1_{TATA}-lacZ</i>	Clontech
Y187	<i>S. cerevisiae</i> MATa, <i>ura3-52, his3-200, ade2-101, trp1-901, leu2-3, 112, gal4D, met^f, gal80D, URA3::GAL1_{UAS}-GAL1_{TATA}-lacZ</i>	Clontech
yPRH-5	HeLa cDNA library in Y187	Clontech
yPRH-11	AH109/ <i>nleF</i> -Gal4 _{DBD} -Myc	This study
Bacterial strains		
EHEC EDL933	wt <i>E. coli</i> O157:H7 isolate	Centers for Disease Control
BL21(DE3)	<i>E. coli</i> F ⁻ <i>ompT hsdSB</i> (r _B ⁻ m _B ⁻) <i>gal dcm</i> (DE3)	Novagen
BL21(DE3)/NleF-FLAG	NleF-FLAG	This study
BL21(DE3)/Tmp21-His	Tmp21-His	This study
BL21(DE3)/NleF-FLAG/Tmp21-His	NleF-FLAG + Tmp21-His coexpression	
XL1-Blue MRF'	$\Delta(mcrA)183 \Delta(mcrCB-hsdSMR-mrr)173$ <i>endA1 supE44 thi-1 recA1 gyrA96 relA1 lac [F' proAB lacI^qZΔM15 Tn10 (Tet^r)]</i>	Stratagene

TABLE 2. PLASMIDS USED IN THIS STUDY.

Plasmid	Genotype or description	Reference
pGBKT7	Yeast Two-hybrid bait plasmid	Clontech
pGADT7	Yeast Two-hybrid library plasmid	Clontech
<i>nleF</i> -Gal4 _{DBD} -Myc	NleF-Gal4-Myc bait plasmid	This study
pBT	Bacterial Two-hybrid bait plasmid	Stratagene
pTRG	Bacterial Two-hybrid target plasmid	Stratagene
sepL-pBT	pBT λ -cl fused to sepL	
NleF-pBT	pBT λ -cl fused to NleF	
sepD-pTRG	pTRG RNAP α fused to sepD	
Tmp21-pTRG	pTRG RNAP α fused to Tmp21	
CD151-pTRG	pTRG RNAP α fused to CD151	
PAIP2a-pTRG	pTRG RNAP α fused to PAIP2	
IFITM1-pTRG	pTRG RNAP α fused to IFITM1	
pFLAG-CTC	Bacterial FLAG fusion protein expression	Sigma
NleF-pFLAG-CTC	NleF-FLAG	[98]
pET28a	Bacterial hexahistidine fusion protein expression	Novagen
Tmp21-pET28a	Tmp21-His	This study
VN	Venus fluorescence protein (AAs 1-173)	This study
VC	Venus fluorescence protein (AAs 155-238)	This study
VN-actin	Venus 1-173 fused to human actin	This study
VC-actin	Venus 155-238 fused to human actin	This study
VN-NleH1	Venus 1-173 fused to NleH1	
VN-NleF	Venus 1-173 fused to NleF	This study
VC-NleF	Venus 155-238 fused to NleF	This study
VC-NleF (1-162)	Venus 155-238 fused to NleF (AAs 1-162)	This study
VC-NleF (1-117)	Venus 155-238 fused to NleF (AAs 1-117)	This study
VC-NleF (1-84)	Venus 155-238 fused to NleF (AAs 1-84)	This study
VC-NleF (1-65)	Venus 155-238 fused to NleF (AAs 1-65)	This study
VN-Tmp21	Venus 1-173 fused to Tmp21	This study
VC-Tmp21	Venus 155-238 fused to Tmp21	This study
VC-Tmp21 (1-180)	Venus 155-238 fused to Tmp21 (AAs 1-180)	This study
VC-Tmp21 (1-150)	Venus 155-238 fused to Tmp21 (AAs 1-150)	This study
VC-Tmp21 (1-124)	Venus 155-238 fused to Tmp21 (AAs 1-124)	This study
VC-Tmp21 (1-63)	Venus 155-238 fused to Tmp21 (AAs 1-63)	This study
pEGFP-VSVG	VSVG in pEGFP-N1	[164]

TABLE 3. OLIGONUCLEOTIDES USED IN THIS STUDY.

Primer	Sequence (5'-3')
NleF XhoI-f-FLAG	GC ₂ TCGAGATGT ₂ AC ₂ A ₂ CA ₂ GTG ₂ T ₂ C
NleF KpnI-r-FLAG	C ₂ GCG ₂ C ₂ GCTC ₂ ACAT ₂ GTA ₃ GATC ₂
NleF EcoRI-f-BT	GATCGA ₂ T ₂ CGATGT ₂ AC ₂ A ₂ CA ₂ GTG ₂
NleF XhoI-r-BT	GATC ₂ TCGAGTCATC ₂ ACAT ₂ GTA ₃ G
NleF NdeI-f-pGBKT7	G ₂ C ₃ ATATGATGT ₂ AC ₂ A ₂ CA ₂ GTG ₂
NleF EcoRI-r-pGBKT7	G ₂ C ₂ GA ₂ T ₂ CTCATC ₂ ACAT ₂ GTA ₃ GATC ₂
NleF XhoI-f-HA	GC ₂ TCGAGATGT ₂ AC ₂ A ₂ CA ₂ GTG ₂ T ₂ C
NleF NotI-r-HA	C ₂ GCG ₂ C ₂ GCTC ₂ ACAT ₂ GTA ₃ GATC ₂
NleF 1-162 NotI-r-HA	C ₂ GCG ₂ C ₂ GCT ₂ C ₂ ACGAG ₂ CAT ₃ CAT ₂ G
NleF 1-117 NotI-r-HA	CGCG ₂ C ₂ GC ₂ AGA ₈ GATC ₃ TGATATA ₂ C
NleF 1-84 NotI-r-HA	C ₂ GCG ₂ C ₂ GCA ₃ TACACTAT ₃ CTCT ₂ ATC ₂
NleF 1-65 NotI-r-HA	C ₂ GCG ₂ C ₂ GCA ₂ T ₃ C ₂ TCA ₂ GCTCAT ₂ AT ₂ AT ₃ C
NleF 1-33 NotI-r-HA	C ₂ GCG ₂ C ₂ GCAT ₂ A ₂ GCTCACT ₂ ACTGAT ₂ C ₃ G ₂
SepL EcoRI-f-BT	GATCGA ₂ T ₂ CGATG ₂ CTA ₂ TG ₂ TAT ₂ G
SepL EcoRI-r-BT	GATC ₂ TCGAGTCACATA ₂ CATC ₂ TC ₂
Tmp21 BamHI-f-His	G ₄ ATC ₂ ATGTCTG ₂ T ₃ GTCTG ₂ C
Tmp21 XhoI-r-His	G ₂ CTCGAGCTCA ₂ TCA ₂ T ₃ CT ₂ G ₂ C ₂
Tmp21 XhoI-f-HA	GC ₂ TCGAGATGTCTG ₂ T ₃ GTCTG ₂ C ₃
Tmp21 NotI-r-HA	C ₂ GCG ₂ C ₂ GC ₂ TCA ₂ TCA ₂ T ₃ CT ₂ G ₂ C ₂
Tmp21 1-180 NotI-r-HA	C ₂ GCG ₂ C ₂ GC ₂ TCGT ₂ G ₂ TATCACGCATCTC ₂
Tmp21 1-150 NotI-r-HA	C ₂ GCG ₂ C ₂ GC ₂ TCTAC ₂ TCTA ₂ TG ₂ T ₃ GAGC
Tmp21 1-124 NotI-r-HA	C ₂ GCG ₂ C ₂ GCTAG ₂ ATCACGAGT ₂ G ₂ TCAG
Tmp21 1-63 NotI-r-HA	C ₂ GCG ₂ C ₂ GC ₂ TG ₂ TCG ₂ AGATCTCGTACG

2.3 Protein Pull Down Assay.

Purified NleF-FLAG and Tmp21-His (~20 μ g), brought up to a final volume of 250 μ l with RIPA buffer (150 mM NaCl, 50 mM Tris pH 8.0, 0.4 mM EDTA, 10 % glycerol, 1 % Nonident P-40 (NP-40)), were applied to 50 μ l ANTI-FLAG M2 resin and incubated with rotation for 5 h at 4 °C. Resins were washed for 10 minutes three times with cold 1X PBS pelleting the resin for 5 minutes of 2,000 g at 4 °C between each wash. Washed resin was resuspended in 30 μ l SDS-PAGE buffer. The samples were separated by SDS-PAGE on a 12 % gel and transferred to nitrocellulose membrane for 1 hour at 100 V. Membranes were blocked with LiCor Odyssey blocking buffer for 1 hour then interrogated for the presence of His-tag with mouse- α -FLAG and rabbit- α -His 1° antibodies (1:1000) overnight at 4 °C. Membranes were washed for 10 minutes 3X at room temperature in PBS-tween then incubated for 30' with Alexa Fluor 680/800 goat- α -rabbit and goat- α -mouse 2° antibodies (1:10000) at room temperature. After a final PBS-tween wash for 20', membranes were imaged with an Odyssey infrared imaging system (Li-Cor).

2.4 Yeast Two-Hybrid Screen.

NleF was cloned into the yeast two-hybrid GAL4 DNA binding domain vector pGBKT7 to generate the 'bait' plasmid. The NleF bait was used to screen a pre-transformed human HeLa cDNA library for proteins interacting with NleF according to the BD Matchmaker Pre-transformed Libraries User Manual (Clontech).

To begin, 50 ml of SD/-Trp broth is inoculated with a fresh 2-3mm colony of the bait strain and incubated at 30 °C to an OD600 of 0.8. The cells are pelleted at 1000 x g for 5 min and the pellet resuspended in 4-5 ml of SD/-Trp to a concentration of $> 1 \times 10^8$ cells per ml. Then 1 ml of library strain is combined with 5 ml of the bait strain in a 2 L flask to which 45 ml of 2X YPDA liquid medium containing 50 ug/ml kanamycin is added. The culture is incubated at 30 °C for 20–24 hr. at 30–50 rpm. The culture is monitored and pelleted at 1000 x g for 10 minutes once the presence of zygotes is confirmed. The pellet is washed in 50 ml 0.5X YPDA containing 50 µg/ml kanamycin then pelleted again at 1000 x g for 10 min then resuspended in 10 ml of 0.5xYPDA/Ken medium. From the mated culture 100 µl of 1/10, 1/100, 1/1,000, 1/10,000 dilutions on are spread on SD/-Trp, SD/-Leo, and SD/-Leo/-Trp (DDO) plates then incubated at 30 °C for 3–5 days. The remaining culture is plated on SD/-Ade/-His/-Leo/-Trp/X-α-Gal (QDO+X-α-Gal) plates and incubated at 30 °C for 3–8 days.

Mating efficiency is calculated as

$$\frac{\text{No. of cfu/ml of diploids}}{\text{No. of cfu/ml of limiting partner}} \times 100 = \% \text{ Diploids}$$

Positive interactions are further analyzed to verify that the interactions are genuine.

Yeast clones, containing library plasmids encoding human proteins interacting with NleF, were purified by restreaking single colonies on QDO/+X- α -Gal plates. Positive blue colonies grow in 2-4 days and are retested for growth phenotypes. Streaking should be performed 2–3 times on DDO/X- α -Gal, each time picking a single blue colony, to increase chances of rescuing the prey plasmid. Yeast cells grown on QDO were used for plasmid rescue to identify the gene responsible for the positive interaction. Since the bait is cloned in pGBKT7, the prey plasmid is selected in LB plus 100 μ g/ml kanamycin. Protein interactions in yeast are verified by cotransformation of 100 ng of each of the following pairs of vectors:

pGBKT7/Bait + Prey in pGADT7

Empty pGBKT7 + Prey pGADT7

and selection on DDO + X- α -Gal and QDO + X- α -Gal plates with incubation for 3–5 days at 30 °C.

Genuine Positives were indicated when blue color was only generated on both selection mediums with bait and candidate prey present. Empty bait vector cotransformed with target preys results in white colonies (DDO + X- α -Gal) or no growth (QDO + X- α -Gal) when bait is not required for reporter gene activation.

Proteins responsible for the interaction were sequenced for identification and β -galactosidase activity was calculated using equation 1: $\beta - gal = (1000 * OD_{420}) / (t * v * OD_{600})$, where t refers to the incubation time [165] and v refers to the concentration factor.

2.5 Bacterial Two-Hybrid Assay.

To verify the proteins identified as interacting partners of the EHEC EDL933 protein NleF subunit, the BacterioMatch two-hybrid system assay was performed with the constructed pBT-NleF. The interactions were evaluated based on the transcriptional activation of the ampicillin resistance reporter gene. Firstly, we transformed 100 μ l of XL1-Blue MRF' reporter strain with 200 ng of pBT-NleF plus 200 ng of a pTRG mammalian target plasmid containing Tmp21, CD151, IFITM1, or PAIP2 α . Transformations were first plated on dual selective screening plates containing 12.5 mg/ml tetracycline and 25 mg/ml chloramphenicol to verify successful co-transformation with both bait and target plasmids. As an interaction positive control, a known interacting protein pair pBT-sepL and pTRG-sepD were used to cotransform the reporter strain and transformation of NleH1-HA-VN was included as a positive control for carbenicillin resistance. pTRG empty vector and recombinant pBT cotransformation served as a negative control. All transformants were selected on 200 mg/ml carbenicillin plates and incubated at 37 °C for 24 h. Growth on carbenicillin plates indicates protein–protein interaction. A schematic of the procedure is presented in Figure 1.

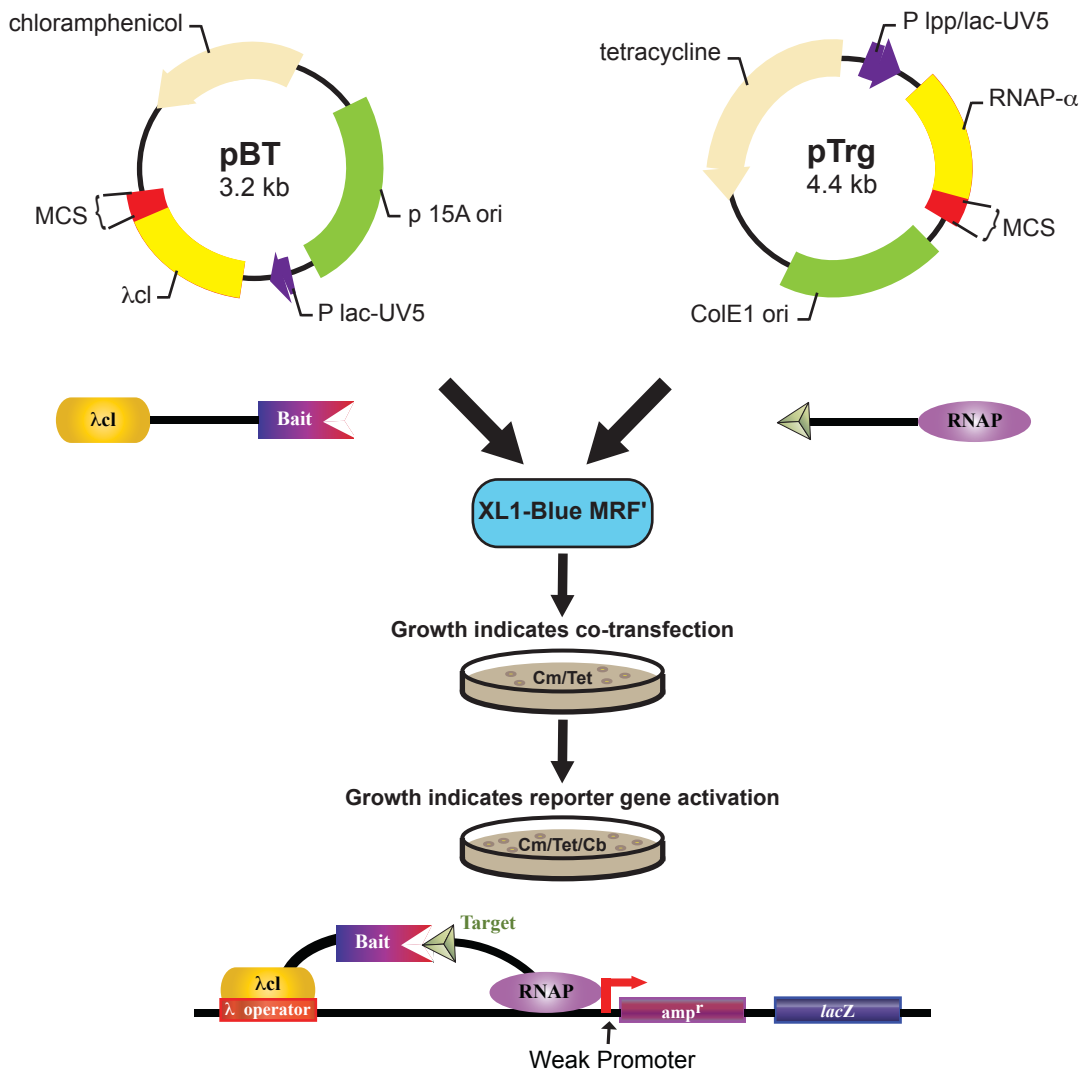


Figure 1. Bacterial Two-Hybrid Assay Schematic.

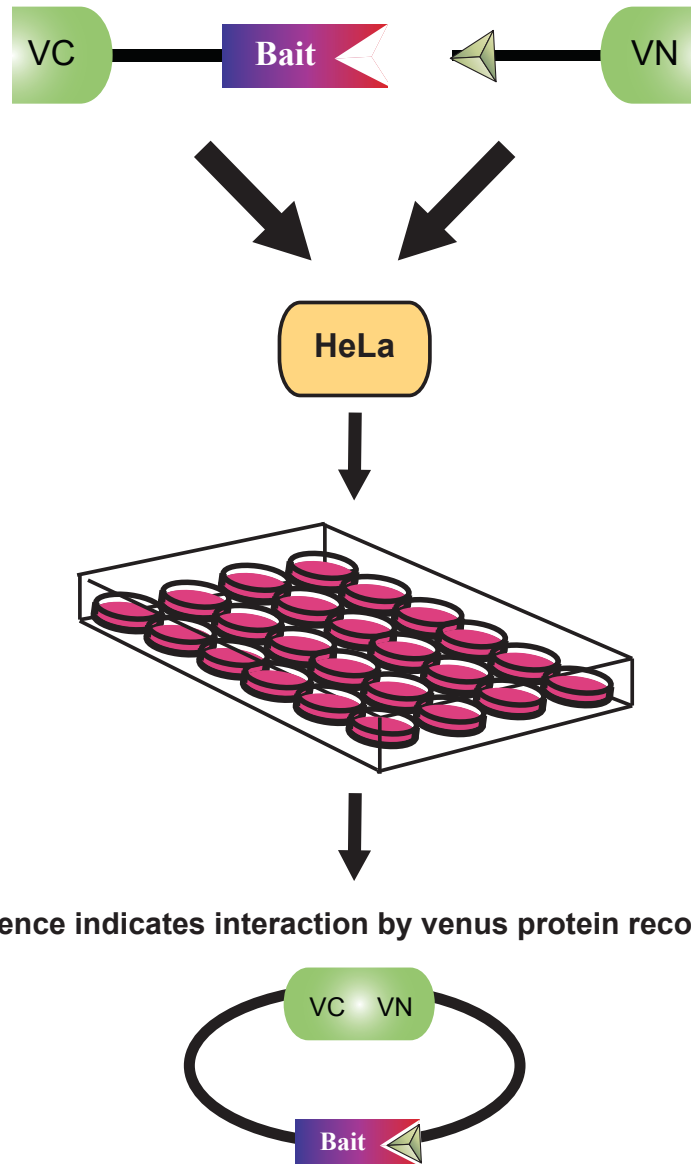
In pBT the first protein ('bait') is fused to full-length λ repressor (λ cl), which binds upstream of a weak promoter to the λ operator. The second plasmid fuses the other protein ('target') to the RNA polymerase α -subunit N-terminal domain (RNAP α). Upon transfection into XL1-Blue MRF' *E. coli*, interaction between bait and target proteins will permit RNA polymerase binding to the weak promoter and subsequent transcription of the reporter gene conferring new resistance to carbenicillin.

2.6 Immunofluorescent detection of co-localization.

HeLa cells were seeded in 24-well cell culture plates (TPP) onto 12 mm glass cover slips and cultured with in RPMI-1640 supplemented with 10 % FBS to a confluence of 40-50 %. Cells were transfected with 1 μ g Tmp21-HA using Transpass HeLa transfection reagent (New England Biolabs). Plasmids was mixed with 50 μ l Opti-MEM and 1 μ l TransPass HeLa then incubated at room temperature for 20-30 minutes. Reaction mixtures were added drop wise to cells and plates were gently swirled. Transfections were incubated for 1 hour at 37 °C in 5 % CO₂ then 500 μ l of complete medium was added to each well and plates were returned to the incubator. Cells were infected with induced *Citrobacter*/pNleF-FLAG 24 hours post-transfection for 4 hours. Cover slips were washed and cells permeabilized with permabilization buffer (1 % goat serum, 0.2 % saponin, 1X PBS) for 10 minutes at room temperature. Samples were incubated with rabbit- α -NleF (1:250) and mouse- α -HA (1:1000) for 2 h at room temperature. Cells were washed 3X 10 minutes with 1X PBS then probed with Alexa Fluor-conjugated secondary antibodies, goat- α -rabbit 488 and goat- α -mouse 568, for 1 h. Coverslips were mounted in Mowiol and samples were visualized using Eclipse 80i fluorescence or Eclipse C1Si confocal microscopes (Nikon).

2.7 Bimolecular Fluorescence Complementation Plasmid construction and Assay.

HeLa cells were seeded in 24-well cell culture plates (TPP) onto 12 mm glass cover slips and cultured with in RPMI-1640 supplemented with 10 % FBS to a confluence of 40-50 %. Cells were co-transfected with two BiFC plasmids (250-500 ng each) representing NleF and Tmp21 truncations cloned as fusions to the N- or C-terminus of Venus eYFP (designated VN and VC) using Transpass HeLa transfection reagent (New England Biolabs). To this end, plasmids were mixed with 50 μ l Opti-MEM and 1 μ L TransPass HeLa then incubated at room temperature for 20-30 minutes. Reaction mixtures were added drop wise to cells and plates were gently swirled. Transfections were incubated for 1 hour at 37 °C in 5 % CO₂ then 500 μ l of complete medium was added to each well and plates were returned to the incubator. Cover slips were washed 24 hours post transfection and cells permeabilized with permabilization buffer (1 % goat serum, 0.2 % saponin, 1X PBS) for 10 minutes at room temperature. Cover slips were mounted onto glass slides with mowiol 4-88 mounting medium. The fluorescence derived from BiFC (due to effector-host protein binding) was visualized using the Eclipse 80i fluorescence microscope (Nikon) and quantified using a fluorescence plate reader with appropriate filters (excitation: 500/20 nm; emission: 535/30 nm). A schematic of the procedure is presented in Figure 2.



Fluorescence indicates interaction by venus protein reconstitution.

Figure 2. Bimolecular Fluorescence Complementation Assay Schematic.

The proteins of interests are attached to either N-terminal or C-terminal fusions with the split Venus fragments, referred to as VN and VC respectively, with a flexible linker region. Here VC is shown fused to the first protein ('bait') and VN to the second protein ('target'). Upon transfection into HeLa cells, association between bait and target proteins will permit reconstitution of the complete Venus protein and subsequent emission of fluorescence.

2.8 Immunoblotting.

HeLa cells were cultured in DMEM supplemented with 10 % FBS and co-transfected with 500–1000 ng plasmid. Cells were lysed in RIPA buffer (150 mM NaCl, 50 mM Tris pH 8.0, 0.5 % sodium deoxycholate, 0.1 % SDS, 1 % Nonident P-40) and incubated on ice for 30'. Lysates were clarified in a 4 °C centrifuge for 5 minutes at 2000 x g. Supernatants were retained for analysis. Samples were resolved on 12 % gels by SDS-PAGE for 1 hour at 200 V. Proteins were transferred to nitrocellulose membranes for 1 hour at 100 V and blocked with Li-Cor Odyssey blocking buffer for 1 hour then interrogated for the presence of HA-tag with mouse- α -HA 1° antibodies (1:1000) overnight at 4 °C to indicate HA-tagged VN or VC expression. Membranes were washed for 10 minutes 3X at room temperature in PBS-tween then incubated for 30' with Ride 680 goat- α -mouse 2° antibody (1:10000) at room temperature. After a final PBS-tween wash for 20', membranes were imaged with an Odyssey infrared imaging system (Li-Cor).

2.9 VSVG Protein Trafficking Assay.

HeLa cells were grown on 12 mm glass coverslips in 24-well tissue culture plates (TPP) to a confluence of 40 % then transfected with Transpass HeLa (New England Biolabs). For transfection only experiments, cells were transfected in 4 replicates with 750 ng VSVG-ts045-YFP alone or co-transfected with 1 μ g NleF-HA-VN. After 24 h, one replicate was left at 37 °C while the other replicates were transferred to 19 °C, 32 °C, or 40 °C incubators. Three hours after temperature shift, cells were rinsed 3 times for 10 minutes with 1X cold PBS then fixed in 3.7 % formaldehyde for 5 minutes at room temperature. Cells were then permeabilized in PBS supplemented with 0.2 % saponin and 1 % goat serum. Samples were blocked with 10 % goat serum in 1X PBS and incubated with primary antibodies for 1 h at room temperature. Cells were washed 3X 10 minutes with 1X PBS then probed with Alexa Fluor-conjugated secondary antibodies for 1 h. Coverslips were mounted in Mowiol and samples were visualized using Eclipse 80i fluorescence or Eclipse C1Si confocal microscopes (Nikon). A schematic of the procedure is presented in Figure 3.

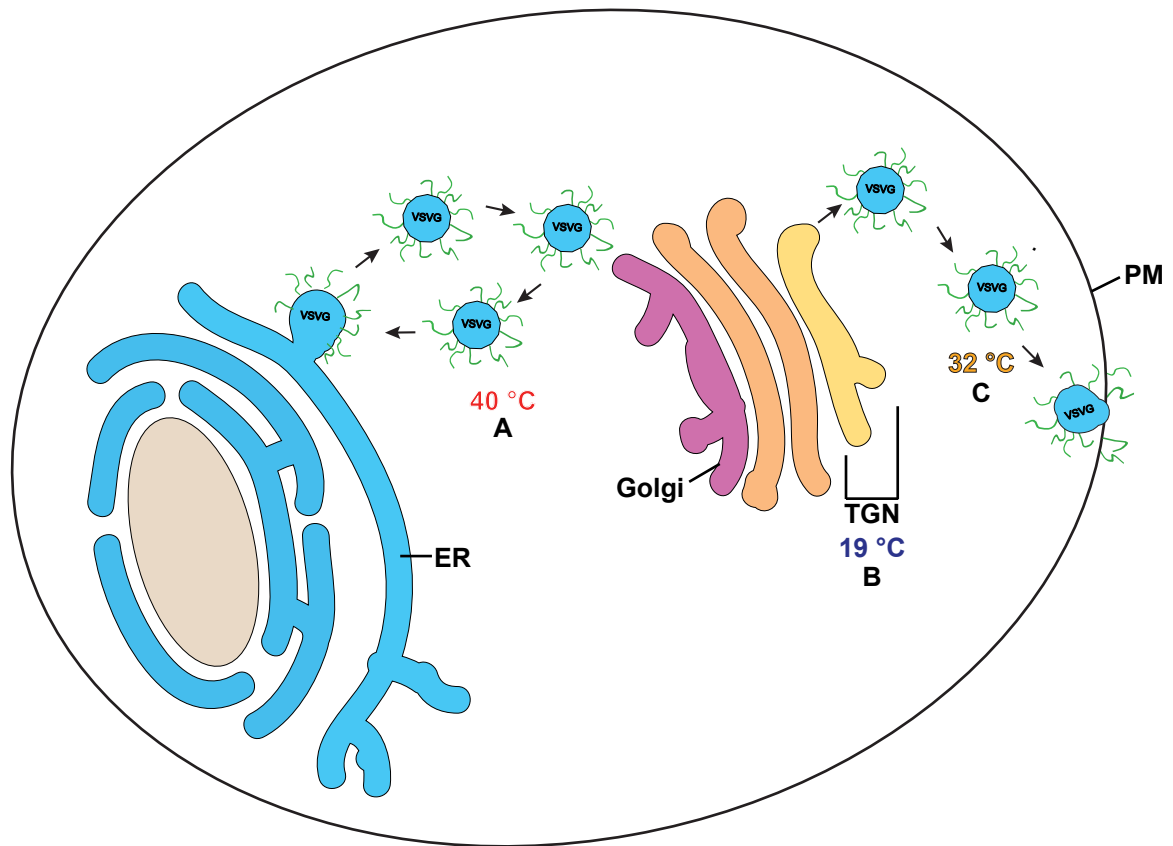


Figure 3. VSVG Trafficking Schematic.

The ts045VSVG (VSVG) follows a known localization pattern based on temperature induced conformational changes. Under physiological conditions (37 °C), ts045VSVG trafficks through the cell moving from Endoplasmic Reticulum to the Golgi and Trans Golgi Network, ultimately reaching the Plasma Membrane. (A) When maintained at 40 °C, the protein is reversibly misfolded resulting in retention in the ER. (B) Temperature shift to 19 °C permits refolding and transit to the TGN. (C) Final temperature shift to 32 °C allows the ultimate transfer to the PM.

2.10 Apoptosis Assay.

Human colorectal adenocarcinoma SW480 cells were seeded on 6-well culture plates for 24 hours for a final confluence of 40 %. To test for the influence of NleF presence on induction of apoptosis, a subset of samples were transfected with 2 $\mu\text{g}/\text{well}$ NleF-HA and incubated for an additional 48 hrs. The cells were then trypsinized in 100 μl Trypsin/EDTA (0.25 % (w/v) trypsin, 0.2 % (w/v) EDTA), 10 μl of each sample was retained for immunoblot verification of NleF expression and the remaining sample brought up to 1 ml in SFM and counted. For staining 1×10^6 cells of each sample were centrifuged down at 2000 x g for 4 minutes. The cells were washed with 1X Annexin V Binding Buffer (0.01 M HEPES, pH 7.4; 1.4 M NaCl; 2.5 mM CaCl_2) and centrifuged again at 2000 x g for 4 minutes, and this was repeated three times. The cell pellets were resuspended in 100 μl Annexin V binding buffer, and 5 μl Annexin V-PE solution (BD Pharmingen, CA, USA) was added. The cells were incubated at room temperature for 15 minutes in the dark then washed 2X and resuspended in 400 μl binding buffer. The cells were analyzed using a BD LSR II flow cytometer (Becton Dickinson). The signal was detected in the 488 nm channel and data analysis was conducted by using the program FACSDiva (Version 6.1.2, Becton Dickinson).

Chapter 3
RESULTS

3.1 Yeast-Two Hybrid Screen and of NleF Mammalian Binding Partners.

To seek targeted mammalian host proteins, we performed a yeast two-hybrid library screen to identify NleF-associated proteins. Using a Gal4-DNA-binding domain (BD)-fused to NleF as bait, we identified a collection of mammalian proteins as NleF binding partners. Yeast harboring the NleF bait and the host protein Tmp21/TMED10 grew under restrictive growth conditions and expressed β -galactosidase (Fig. 4). Additional host proteins were identified as NleF-associated including CD151, IFITM1, and PAIP2 α (data not shown), but we chose to focus on Tmp21 for this study.

3.2 Bacterial-Two Hybrid Verification of NleF Mammalian Binding Partners.

We conducted a bacterial two-hybrid screening assay to verify the potential NleF interactions identified by the yeast two-hybrid screen. In the bacterial two-hybrid screening, we verified interaction with four of the proteins identified in the earlier screen, including NleF/Tmp21, NleF/CD151, NleF/IFITM1 and NleF/PAIP2 α . All interactions and controls are indicated in Table 4.

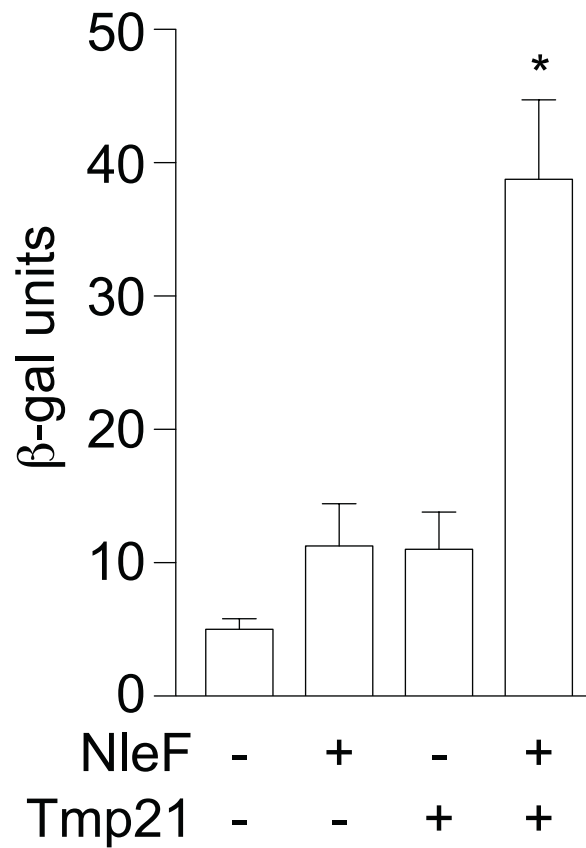


Figure 4: Measurement of NleF binding to Tmp21 with the β-galactosidase assay.

NleF was expressed in yeast in the presence or absence of human Tmp21 and β-galactosidase activity was quantified. Asterisks indicate significantly different β-galactosidase activity as compared with untransformed yeast ($p < 0.05$ t-test).

TABLE 4. BACTERIAL TWO-HYBRID ANALYSIS OF POTENTIAL PROTEIN-PROTEIN INTERACTION BETWEEN NLEF AND IDENTIFIED MAMMALIAN PROTEINS.

Target Protein (pTRG)	Protein					
Bait Protein (pBT)	pTRG empty	sepD 2348/69	Tmp21/TMED10 (human) ORF	CD151 (human) ORF	IFITM1 human ORF)	PAIP2a (human ORF)
pBT	-	-	-	-	-	-
sepL 2348/69	-	+	-	-	-	-
NleF EDL933	-	-	+	+	+	+

E. coli XL-1 Blue MRF' containing the indicated plasmid combinations were assessed for positive interactions (+) or no interaction (-).

3.3 Co-immunoprecipitation of NleF and Tmp21.

We expressed and purified recombinant forms of NleF-FLAG and Tmp21-His in *E. coli* BL21(DE3). We then used the purified proteins in pull-down assays, which confirmed that IP of NleF-FLAG also pulls down Tmp21-His, indicating the proteins interact directly *in vitro* (Fig. 5).

3.4 NleF and Tmp21 Co-localize.

To explore an interaction between NleF and Tmp21, we first verified effective detection of NleF after translocation into HeLa cells during *E. coli* infection using an antibody we generated against NleF protein in rabbits [98]. The specificity of the polyclonal antibody was tested on HeLa cells infected with *Citrobacter/pNleF-FLAG*. The antiserum detected NleF in infected HeLa cells but not uninfected controls (Fig. 6A), indicating both specific labeling and successful translocation of NleF.

HA-tagged Tmp21 was then transfected in HeLa cells cultured in serum-supplemented RPMI-1640. After 24 h, cells were infected with induced *Citrobacter/pNleF-FLAG* for 4 hours. The intracellular co-localization of NleF and HA-tagged Tmp21 were determined by confocal immunofluorescence microscopy. Co-staining for Tmp21 revealed that both proteins were detected and colocalized in a perinuclear location, likely the ER/TGN (Fig. 6B).

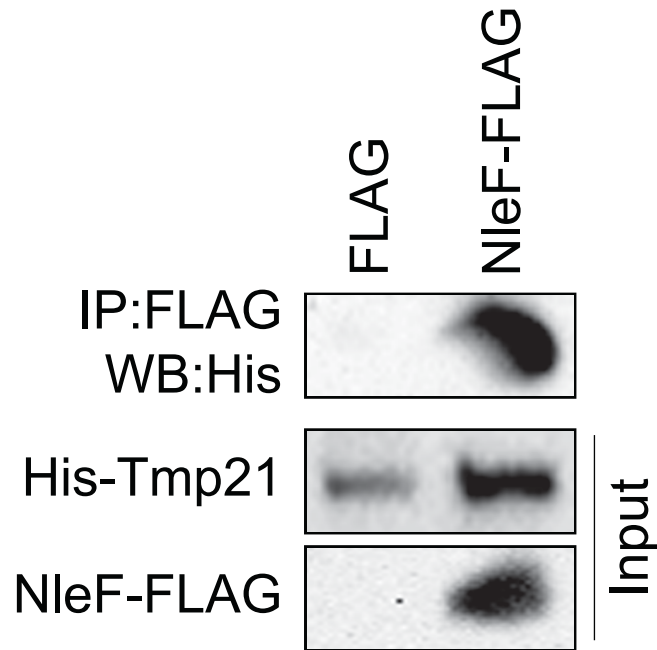


Figure 5: Tmp21 is immunoprecipitated with NleF.

Tmp21 was cloned into pET28a to generate His-Tmp21 and was co-expressed with NleF-FLAG in *E. coli* BL21(DE3). NleF was immunoprecipitated and binding of His-Tmp21 was assessed using immunoblotting.

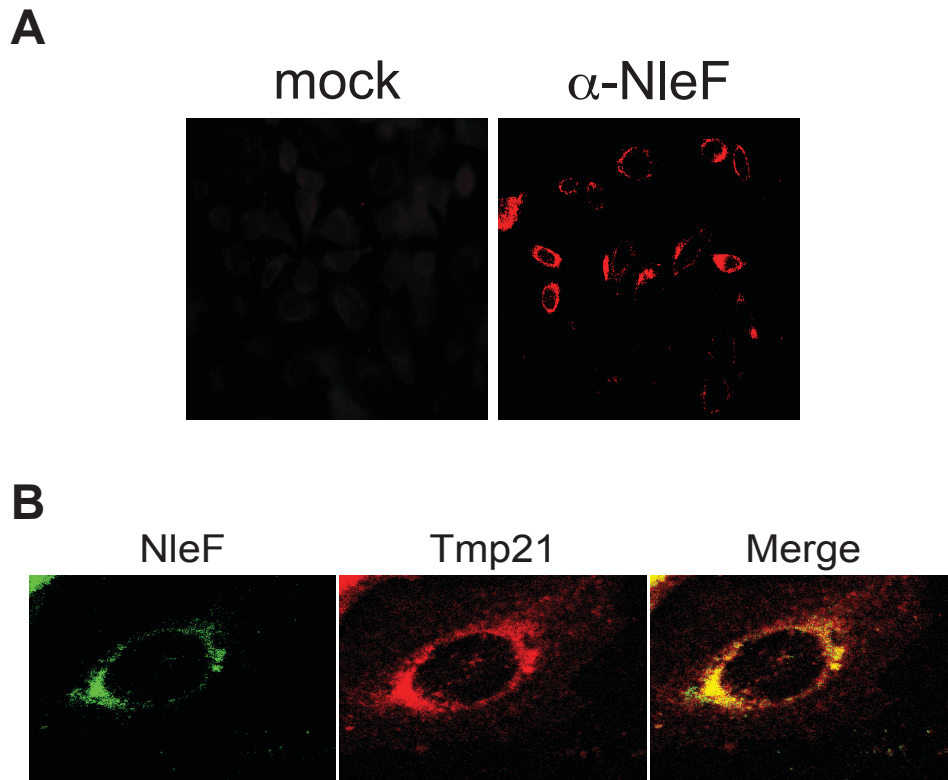


Figure 7: NleF and Tmp21 co-localize in HeLa Cells.

(A) HeLa cells were infected with *Citrobacter/pNleF-FLAG* and stained with α -NleF (red) to detect NleF translocation. (B) HeLa cells were transfected with Tmp21-HA then infected with *Citrobacter/pNleF-FLAG*. Cells were stained with both an α -NleF (green) and α -HA (red).

3.5 Bimolecular Fluorescent Complementation Analysis supports interaction of NleF and Tmp21.

We used bimolecular fluorescence complementation (BiFC) assays to ascertain if NleF and Tmp21 interact in mammalian cells when co-expressed. Plasmids fusing NleF and Tmp21 with eYFP N- and C-terminal fragments VN and VC were constructed and expression verified (Fig 7A). N and C-terminal chimeras of actin were included as a positive control. Interaction of the proteins was indicated by reconstitution of YFP fluorescence upon co-expression. Comparable intensity of fluorescence signal between the actin control and the NleF/Tmp21 combinations further corroborates NleF binds to Tmp21 in mammalian cells (Fig. 7B). Mapping of the binding domain through co-expression of NleF and Tmp21 truncation combinations demonstrated amino acids 1-84 of NleF and 63-180 of Tmp21 are required for interaction. Loss of fluorescence supports NleF C-terminal association with the C-terminal region of Tmp21 (Fig 9).

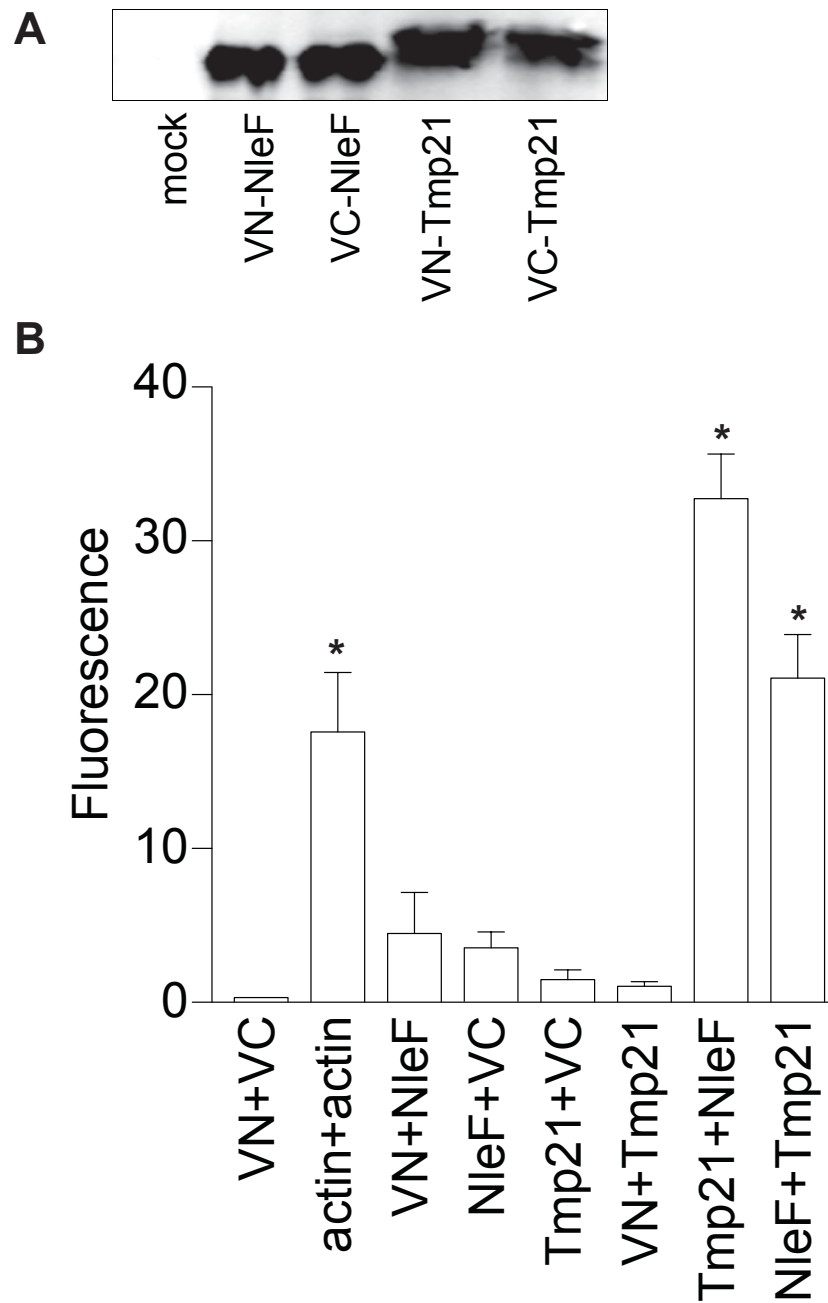


Figure 7: Full Length NleF and Tmp21 Expression and Fluorescence Quantification.

(A) NleF and Tmp21 were cloned into eYFP-VN and eYFP-VC vectors and protein expression was verified by immunoblotting. (B) Relative fluorescent intensity after cotransfection indicated NleF- and Tmp21-eYFP plasmid combinations (n=3). Asterisks indicate significantly different fluorescence intensity as compared with transfected samples ($p < 0.05$, ANOVA).

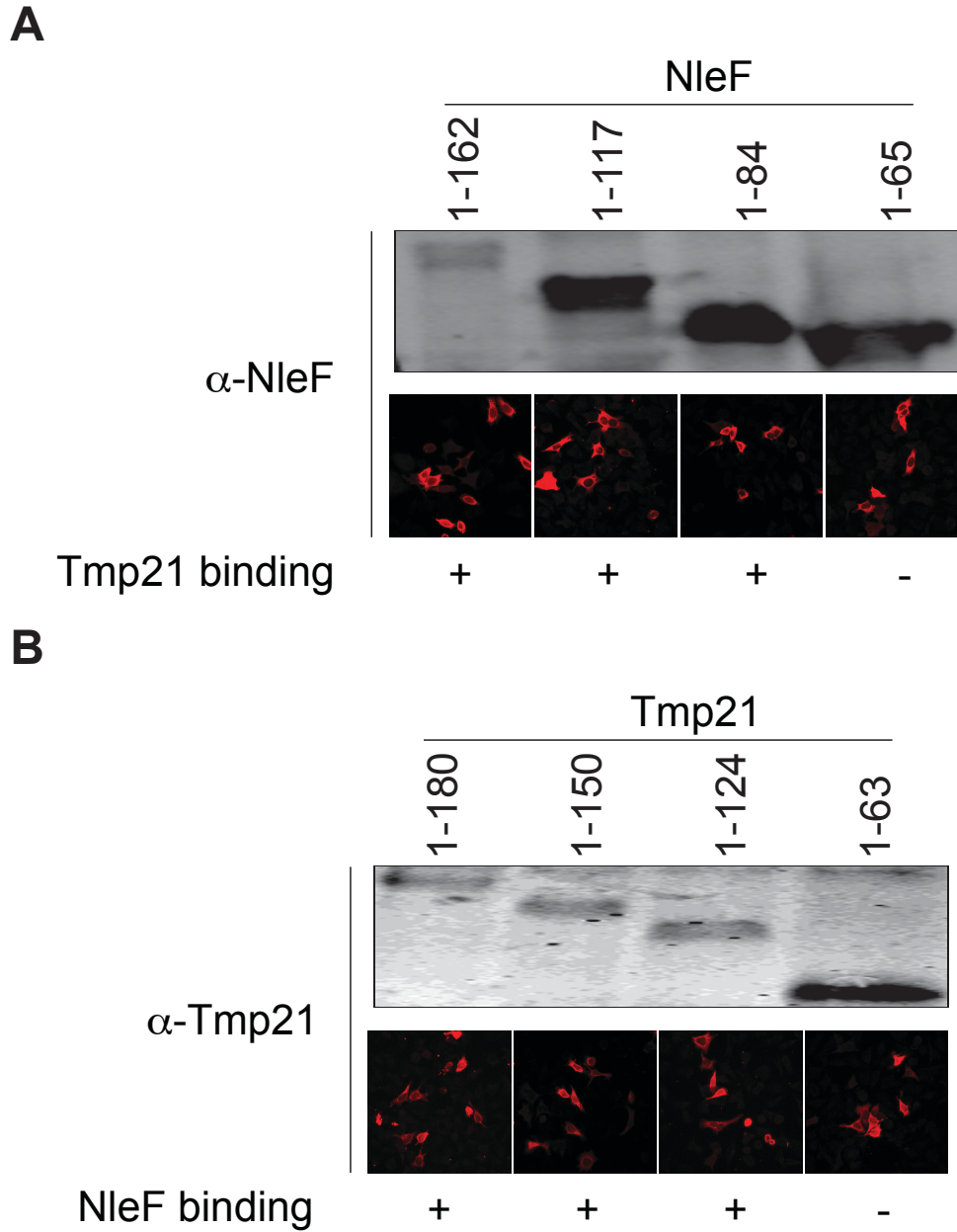


Figure 8: NleF and Tmp21 Truncation Expression and interaction verification.

NleF truncations (A) and Tmp21 truncations (B) were cloned into eYFP-VC vectors protein expression was verified by immunoblotting and immunofluorescence. Binding to Tmp21-eYFP-VN (A) and NleF-eYFP-VN (B) were measured using BiFC and scored as positive (+) or negative (-) in the respective columns.

3.6 NleF Alters VSVG-GFP trafficking.

HeLa cells were transfected with pVSVG-EGFP and VSVG localization determined by immunofluorescence microscopy. HA staining revealed cytosolic or PM localization in controls, verifying NleF, and not the HA-tag, was responsible for the observed localization in samples (Fig 9). As expected, when cells were shifted from 37 °C to 40 °C, VSVG-GFP fluorescence became localized primarily in the ER, as revealed by its colocalization with the ER protein calnexin (Fig. 10). As described in previous studies, when cells were subsequently shifted to 19 °C, VSVG localization with calnexin was lost and VSVG was primarily redistributed to the Golgi as signified by its colocalization with the Golgi protein golgin-97 (Fig. 11) [164]. Incubating cells at 32 °C also resulted in the expected subsequent shift of VSVG from the Golgi to the PM (data not shown).

After transfecting (Fig. 10) or infecting (Fig. 12) HeLa cells with NleF and performing temperature shift experiments, we observed VSVG mislocalization to the ER rather than the Golgi at 19 °C in 74 % of cells examined ($p < 0.05$, Fisher's exact test, Fig. 10). Similarly, NleF presence resulted in VSVG being mislocalized to the Golgi at 32 °C in 58 % of cells examined ($p < 0.05$, Fisher's exact test, Fig. 11).

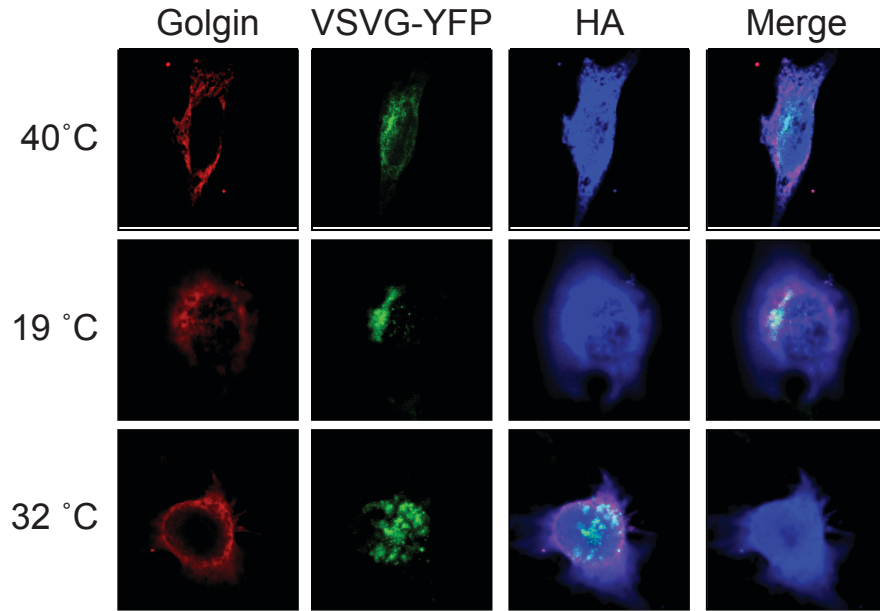


Figure 9: Verification of HA control staining in HeLa Cells.

HeLa cells were transfected with VSVG-GFP and HA-VN then shifted to 19 °C, 32 °C, or 40 °C. Cells were stained with both an α -golgin-97 (red) and α -HA (blue).

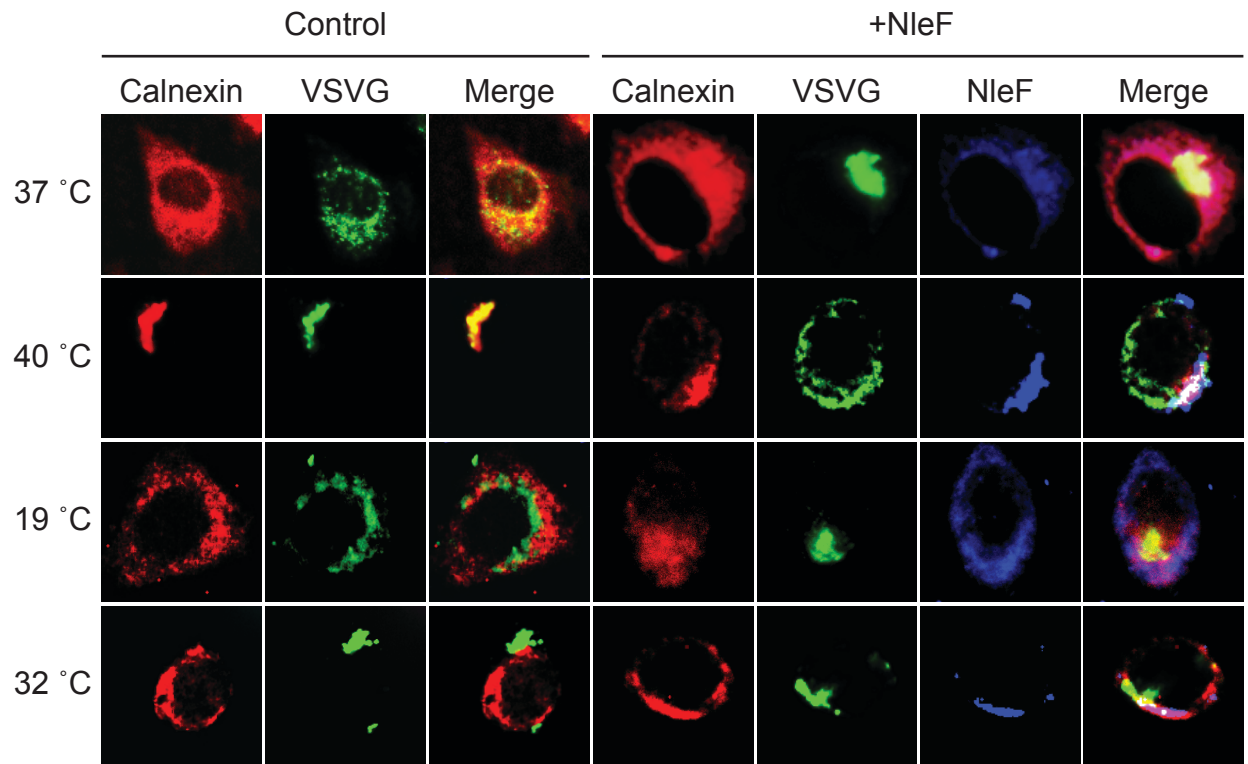


Figure 10: NleF alters VSVF-GFP trafficking in reference to the endoplasmic reticulum when delivered by transfection.

HeLa cells were transfected with VSVG-GFP alone (controls) or with NleF-HA-VN (+NleF) then incubated at 37 °C or shifted to 19 °C, 32 °C, or 40 °C for 3 hours. Cells were stained with both α -Calnexin (red) and α -HA (blue).

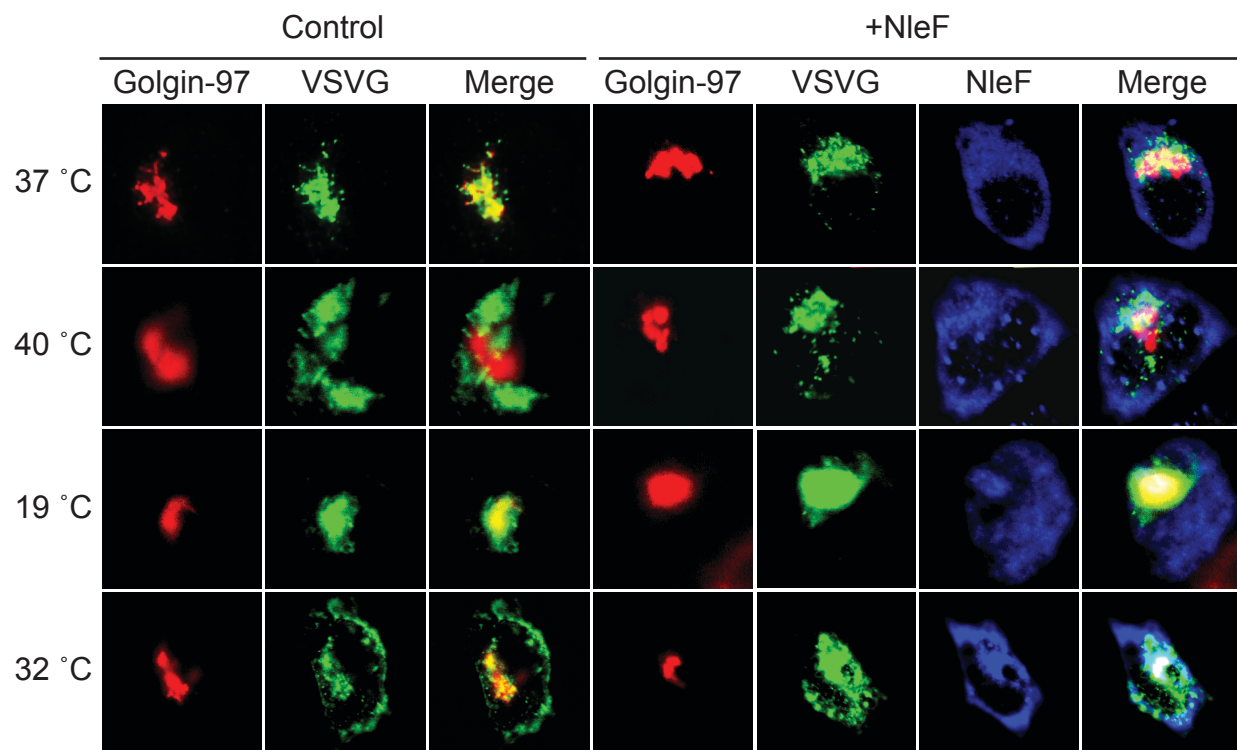


Figure 11: NleF alters VSVF-GFP trafficking in reference to the Golgi when delivered by transfection.

HeLa cells were transfected with VSVG-GFP alone (controls) or with NleF-HA-VN (+NleF) then incubated at 37 °C or shifted to 19 °C, 32 °C, or 40 °C for 3 hours. Cells were stained with both α -golgin-97 (red) and α -HA (blue).

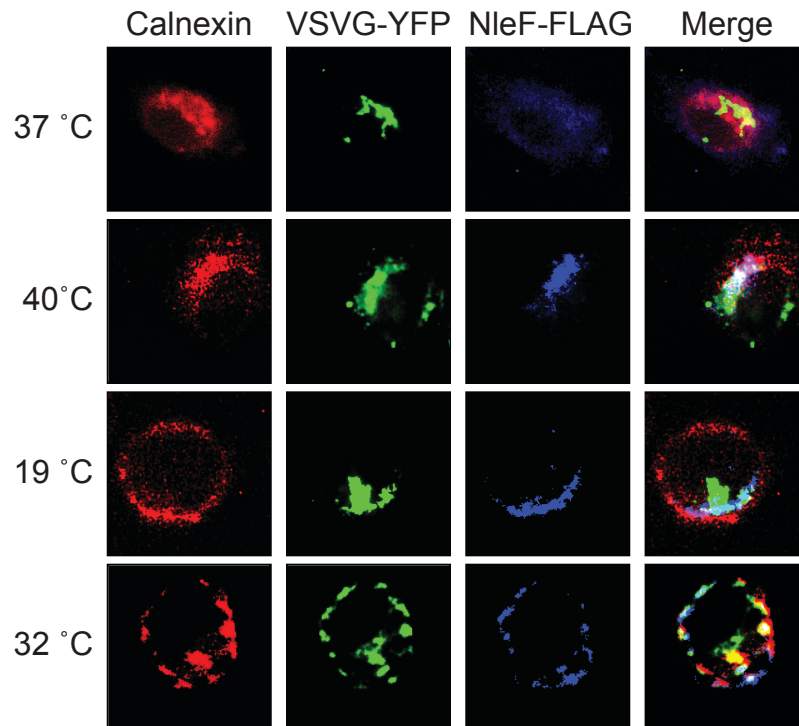


Figure 12: NleF alters VSVF-GFP trafficking when delivered by infection.

HeLa cells were transfected with VSVG-GFP and incubated overnight. *Citrobacter rodentium* harboring an NleF-FLAG vector were cultured overnight, subcultured 1:100, and protein expression was induced with 1 mM IPTG. After initiation of induction, transfected HeLa cells were infected with the culture then shifted to 19 °C, 32 °C, or 40 °C and incubated for 2 hours. Cells were washed to remove adherent bacteria then fixed and stained with both α -Calnexin (red) and α -HA (blue).

3.7 NleF does not Induce Apoptosis in Mamalian Colorectal Cancer Cells.

Wang et. al. demonstrated Tmp21 is involved in induction of apoptosis through interaction with the C1b domain of protein kinase C delta (PKC δ). RNAi knock down of Tmp21 and mutational disruption of the interaction in LNCaP prostate cancer cells resulted in enhanced PKC δ -dependent apoptosis and activation of down stream effectors ROCK and JNK. Depletion of Tmp21 also led to an increase in PKC δ translocation to the PM. Taken together, Wang et. al. identify Tmp21 as an anchoring protein that blocks PKC δ activation of apoptosis through perinuclear retention away from stimuli [163]. As we have established NleF binds Tmp21, we sought to determine if that interaction altered the ability of Tmp21 to block induction of apoptosis. To this end, we considered the influence of NleF presence on cell death in cancer cells, which have a natural resistance to apoptosis. We measured Annexin-V binding of phosphatidylserine (PS) as an established indicator of apoptosis. Exposure of PS occurs early in apoptosis onset and Annexin V has strong binding affinity for PS when calcium is present. SW480 cells were transfected with NleF-HA and cells were stained with Annexin V-PE to assess the effect of NleF on induction of apoptosis in a colorectal cancer cell line under normal conditions (Fig. 13). Annexin V antibody binding revealed that basal apoptosis in the untreated culture was 4.4 %, which increased to a mere 8 % with expression of NleF. Based on this data, NleF did not visibly alter apoptosis levels, suggesting NleF does not influence the typical Tmp21 association with PKC δ .

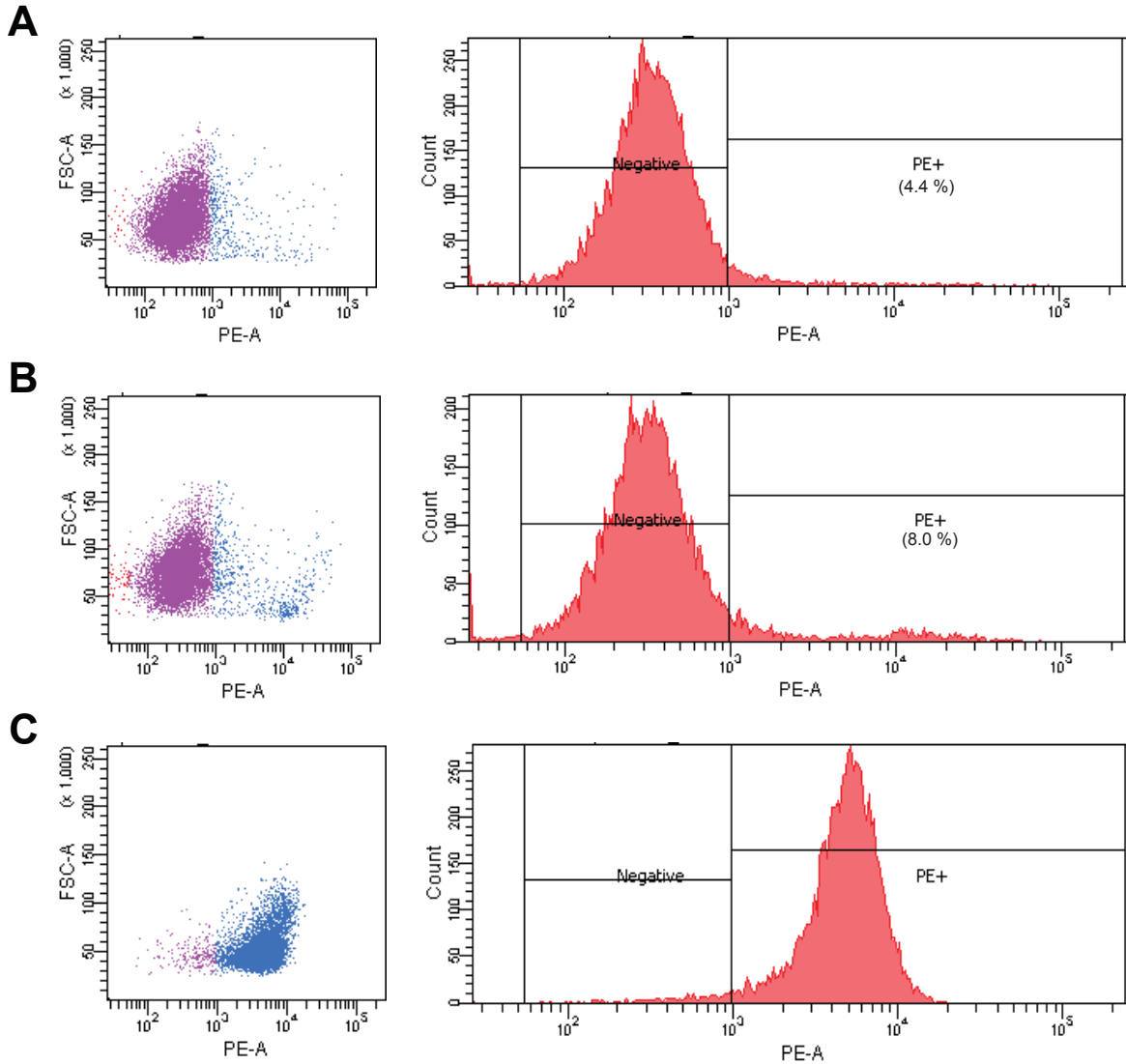


Figure 13: NleF does not induce apoptosis in colorectal adenocarcinoma cells.

Human SW480 cells were transfected, harvested and labeled with Annexin V-PE, and analyzed by flow cytometer. Histograms present Annexin-V binding (PE+) of 4.4 % transfection-treated control cells (A), 8.0 % cells transfected with 2 μg NleF-HA (B) and cells treated with MeOH prior to flow analysis as a positive control (MeOH = 100 %). Flow analysis results indicate apoptosis is not induced by the presence of NleF-HA. Values are percentage PE+ cells.

Chapter 4
DISCUSSION

We conducted a yeast two-hybrid (Y2H) screen to determine the mammalian binding partners of NleF. We identified several mammalian proteins as putative NleF binding partners. We also performed a bacterial two-hybrid assay, which also verified the interactions identified in the Y2H assay. Here we chose to focus on Tmp21 (also named p23/p24d/TMED10) and confirmed the interaction using direct Y2H assays and by quantifying β -galactosidase activity resulting from NleF-Tmp21 co-expression. As NleF demonstrates the ability to associate with numerous other mammalian proteins, further investigation will be required for those supposed interactions. Here we focused on verification of Tmp21/TMED10 interaction and elucidation of the consequences of this interaction in the host.

Tmp21 is a 219 amino acid integral type I transmembrane protein that functions as an integral receptor for the COPI-vesicle coat [144]. Tmp21 is a member of the p24 (p24/gp25L/emp24/Erp) protein family. These proteins provide cargo receptors to proteins and regulate protein packaging into COPI vesicles in concert with a small GTPase, the ADP-ribosylation factor 1 (Arf1) [166]. p24 proteins are assembled into heteromeric complexes that cycle between the ER and the Golgi and recruit Arf1 in early stages of vesicle formation [167]. p24 proteins thus play active roles in retrograde protein transport from Golgi to ER by facilitating the formation of COPI-coated vesicles [168].

By expressing and purifying recombinant forms of NleF and Tmp21 in *E. coli* BL21(DE3) and then using these proteins in pull-down assays, we were also able to confirm that NleF and Tmp21 interact directly *in vitro*. Additionally, we used immunofluorescence

microscopy to determine the extent of NleF-Tmp21 colocalization by generating a polyclonal α -NleF antibody and using this antibody to detect NleF after its translocation into HeLa cells during *E. coli* infection [169]. Co-staining for Tmp21 revealed that both proteins were detected and colocalized in a perinuclear location.

To determine whether NleF and Tmp21 interact when they are co-expressed in mammalian cells, we used bimolecular fluorescence complementation (BiFC) assays. We generated protein chimeras with split N- and C-terminal fragments (VN and VC, respectively), of eYFP fused to either NleF or Tmp21. Co-expressing eYFP chimeras of Tmp21 and NleF reconstituted YFP fluorescence, to a similar magnitude as the actin positive control, whereas transfecting individual plasmids did not reconstitute YFP fluorescence, suggesting that NleF binds to Tmp21 in mammalian cells.

The N-terminal luminal domain of Tmp21 mediates cargo uptake into transport vesicles, whereas the KKLIE cytoplasmic tail at the Tmp21 carboxy-terminus mediates COPI-dependent transport vesicle formation [170]. To map the binding domain of NleF on Tmp21, we carried out a structure-function study with C-terminal deletions of NleF. BiFC experiments revealed that deleting the NleF C-terminus beyond amino acid 84 eliminated NleF binding to full length Tmp21, indicated by loss of fluorescence with sequential truncated constructs. A similar IP analysis revealed that the C-terminal region of Tmp21, amino acids 63-180, was required for binding to NleF. Thus, the data support association of the C-terminal regions of NleF and Tmp21.

We tested the hypothesis that NleF binding to Tmp21 causes protein trafficking defects by characterizing the localization of a temperature-sensitive vesicular stomatitis virus glycoprotein (VSVG) as a function of NleF presence and temperature. VSVG localization is commonly used to study mammalian protein trafficking [171]. This glycoprotein is essential for viral envelope fusion with the host PM and traffics intracellularly via the ER and Golgi [172]. This system has been employed successfully in studies of *Salmonella*-mediated disruption of host exocytic transport [101].

Immunofluorescence microscopy evaluation of pVSVG-EGFP localization in transfected HeLa cells was employed. The transport of a temperature-sensitive VSVG-GFP mutant, VSVG-ts045, can be synchronized through exposure to different temperatures [98]. Sub-cellular position in controls matched the VSVG-ts045 trafficking model previously established with localization in the ER at 40 °C the Golgi at 19 °C, and the PM at 32 °C. If incubated at 40 °C, VSVG-ts045 becomes reversibly misfolded and retained in the ER. If shifted to 19 °C, VSVG-ts045 refolds and can be transported to the TGN. A further temperature shift to 32 °C allows subsequent VSVG-ts045 trafficking to the PM.

NleA is known to block anterograde transport by COPII inclusive vesicles through binding to sec24, a component of the COPII heterodimer, and disrupting interactions required for anterograde trafficking. As Tmp21 binds COPI, we predicted that NleF interaction with Tmp21 would similarly result in disruption of COPI-mediated transport leading to a delay or block in retrograde trafficking (Fig. 15). Colocalization of VSVG-EGFP and the ER at 19 °C indicates retrograde vesicle trafficking or reduction in anterograde trafficking occurs in the presence of NleF (Fig. 11). Further evidence of

altered trafficking was found by visible colocalization of VSVG-EGFP and the Golgi at 32 °C and 40 °C with golgin-97 staining (Fig. 12). These results support continued trafficking in both the anterograde and retrograde directions with NleF present.

One of the known binding partners of Tmp21 is mammalian PKC δ . As mentioned previously, the consequences of this interaction have been shown to result in reduced or blocked cellular apoptosis [163]. If interaction between Tmp21 and NleF occurs in the same region as Tmp21 interaction with PKC δ , we predicted NleF presence could impede Tmp21 perinuclear anchoring of PKC δ resulting in induction of apoptosis. As a preliminary enquiry into the effects of the NleF and Tmp21 interaction on apoptosis levels, we considered the outcome of NleF presence on the induction of cell death in colorectal cancer cells. Since the uncontrolled growth of cancer cells is partially dependent on their ability to resist apoptosis, we anticipated an increase in apoptosis as a result of NleF expression would support interference in the demonstrated interaction between Tmp21 and PKC δ . Conversely, apoptosis remained at levels comparable to controls regardless of NleF presence. This would suggest the association with Tmp21 is not sufficient to alter cell death in the cancer line. There are numerous explanations for the lack of apoptosis induction if this were the case. The location of NleF-Tmp21 interaction may be in a position that does not obstruct the interface and orientation between Tmp21-PKC δ . NleF may only hinder a pool of the total cellular Tmp21, thus allowing sufficient unbound Tmp21 to reach PKC δ . Just as likely, the continued resistance to apoptosis could be dependent on a completely unrelated pathway or protein that is too substantial to be overcome by our interaction. However, it is important to consider the significance of our data is limited. Determining statistical relevance is not

possible as the assay was performed only once (n=1) and additional replicates would be required to verify significance. Furthermore, the MeOH positive control does not induce apoptosis, but rather permeabilizes the cells. This exposes PS and permits Annexin-V binding, as indicated by the intense PE+ signal (Figure 13), but does not imply apoptosis is occurring. Therefore, the level of induction assumed by the MeOH control is not an accurate indicator of real levels observed upon induction of apoptosis. Use of a known inducer of apoptosis, such as etoposide, would be a superior choice for a positive control. Finally, the NleF+ sample was not tested for transfection efficiency. Though immunoblot verified expression of NleF in the SW480 cells after transfection and prior to processing for the Annexin-V assay (data not shown), the percentage of the population expressing NleF and the level of expression was not determined. For this reason, the observed intensity could be indicative of a significant induction of apoptosis by NleF if only a small percentage of the cells were expressing NleF. As a result, interpretation of the data could be underestimating the influence of NleF. Further investigation into the potential role of NleF in apoptosis with improved controls and expression verification should be performed to eliminate these issues.

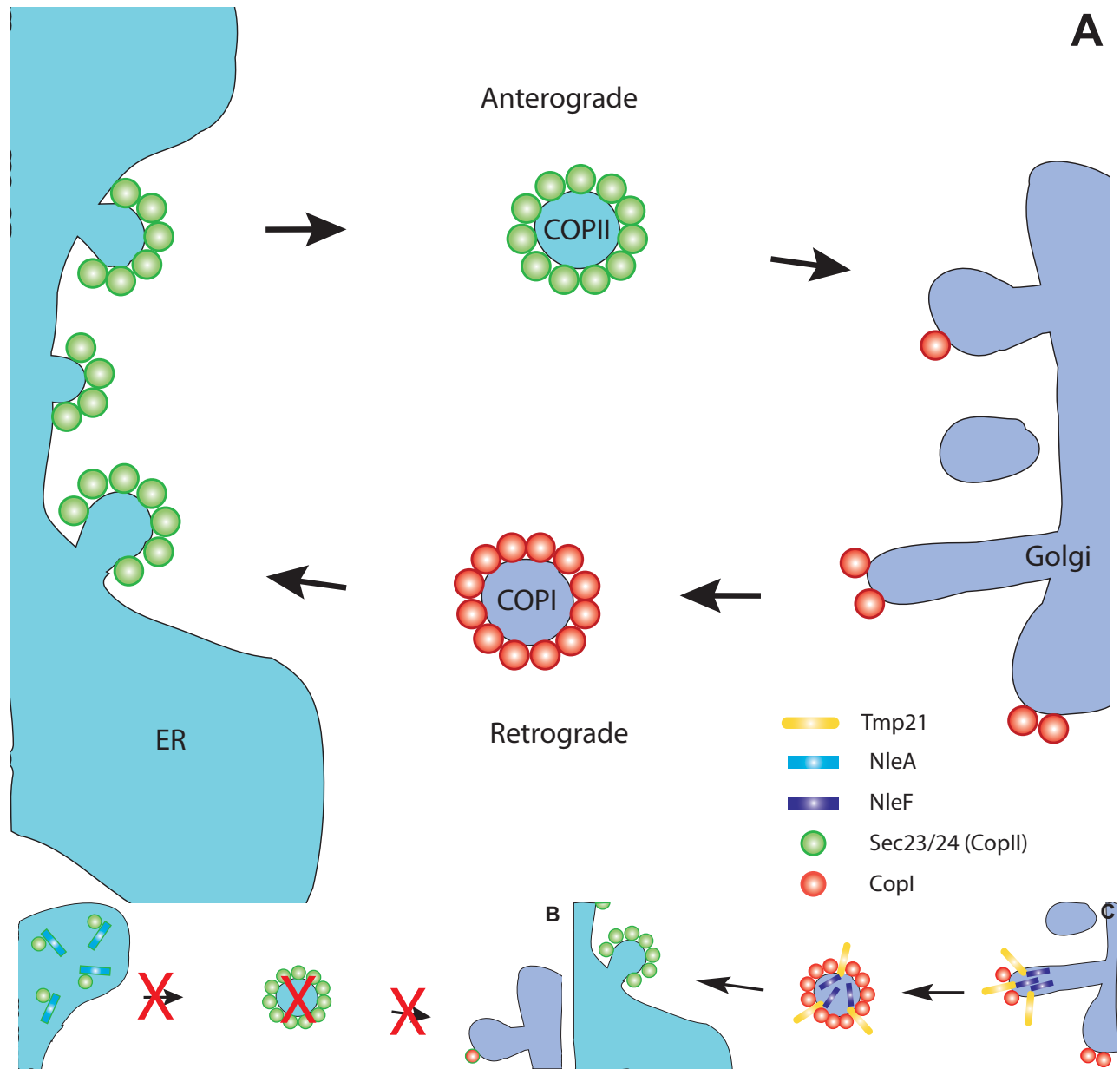


Figure 14: EHEC effector protein alteration of trafficking.

The early steps in the mammalian protein secretion pathway are based on membrane composition. COPII (anterograde) or COPI (retrograde) membrane coats dictate the direction of vesicle movement (A). NleA obstructs anterograde transit through interaction with COPII coat member Sec24 resulting in block of vesicle budding (B). VSVG assay data reveal NleF influences COPI transit through interaction with Tmp21, by an unknown mechanism, leading to slowed anterograde trafficking (C).

Overall, our data support an interaction between NleF and Tmp21 by yeast two-hybrid verification, bacterial two-hybrid, immunoprecipitation, and BiFC analysis. However, further characterization of the regions involved in this interaction is necessary. Furthermore, our results indicate NleF binding causes altered vesicular trafficking in the context of the tsVSVG trafficking model system. While these results point to a role for NleF in altering typical vesicle trafficking patterns, they do not consider such effects from the perspective of the NleF interaction with Tmp21. Additional experiments measuring NleF influence specifically on Tmp21 localization should be carried out to fully characterize the outcome of this interaction in the host. Lastly, while we expected the interaction between Tmp21 and PKC δ might be sufficiently altered by NleF-Tmp21 binding leading to an increase in induction of apoptosis, our results did not support increased cell death. Further inquiry into the consequences in relation to cell death should be pursued in order to determine if our identified interaction represents the most crucial host target by NleF, or if another target is more pertinent to virulence.

Chapter 5
REFERENCES

1. CDC, *Escherichia coli (E. coli): General Information*, CDC, Editor 2012.
2. Deng, W., et al., *Dissecting virulence: systematic and functional analyses of a pathogenicity island*. Proceedings of the National Academy of Sciences of the United States of America, 2004. **101**(10): p. 3597-602.
3. Rangel, J.M., et al., *Epidemiology of Escherichia coli O157:H7 outbreaks, United States, 1982-2002*. Emerging infectious diseases, 2005. **11**(4): p. 603-9.
4. *E. Coli: General Information*. 2012 August 3, 2012.
5. Schiller, L.R. and J.H. Sellin, *Diarrhea*, in *Sleisenger & Fordtran's Gastrointestinal and Liver Disease*, F. M, L. Friedman, and L. Brandt, Editors. 2012, Saunders Elsevier: Philadelphia.
6. Sodha, S.V., G. P.M., and H. J.M., *Foodborne Diseases*, in *Principles and Practice of Infectious Diseases*. , G.L. Mandell, J.E. Bennett, and R. Dolin, Editors. 2009, Elsevier Churchill Livingstone: Philadelphia.
7. Craig, S.A. and D.K. Zich, *Gastroenteritis*, in *Rosen's Emergency Medicine: Concepts and Clinical Practice*. , J.A. Marx, Editor 2009, Mosby Elsevier: Philadelphia.
8. *Bacterial gastroenteritis*, in *A.D.A.M. Medical Encyclopedia*, L.J. Vorvirk, G.F. Longstreth, and D. Zieve, Editors. 2011, PubMed Health: Atlanta (GA).
9. Pennington, H., *Escherichia coli O157*. Lancet, 2010. **376**(9750): p. 1428-35.
10. Tarr, P.I. *Escherichia coli O157:H7: A malevolent mosaic*. in *Proceedings of the Pathogenic E.coli Network Conference Epidemiology and Transmission of VTEC and other Pathogenic Escherichia coli*. 2008. Stockholm.
11. Tarr, P.I., C.A. Gordon, and W.L. Chandler, *Shiga-toxin-producing Escherichia coli and haemolytic uremic syndrome*. Lancet, 2005. **365**(9464): p. 1073-86.
12. Holtz, L.R., M.A. Neill, and P.I. Tarr, *Acute bloody diarrhea: a medical emergency for patients of all ages*. Gastroenterology, 2009. **136**(6): p. 1887-98.
13. Nguyen, Y. and V. Sperandio, *Enterohemorrhagic E. coli (EHEC) pathogenesis*. Frontiers in cellular and infection microbiology, 2012. **2**: p. 90.
14. Karch, H., et al., *Shiga toxins even when different are encoded at identical positions in the genomes of related temperate bacteriophages*. Molecular & general genetics : MGG, 1999. **262**(4-5): p. 600-7.
15. Matsushiro, A., et al., *Induction of prophages of enterohemorrhagic Escherichia coli O157:H7 with norfloxacin*. Journal of bacteriology, 1999. **181**(7): p. 2257-60.
16. Wagner, P.L., et al., *Bacteriophage control of Shiga toxin 1 production and release by Escherichia coli*. Molecular microbiology, 2002. **44**(4): p. 957-70.
17. Karmali, M.A., V. Gannon, and J.M. Sargeant, *Verocytotoxin-producing Escherichia coli (VTEC)*. Veterinary microbiology, 2010. **140**(3-4): p. 360-70.
18. Koster, F., et al., *Hemolytic-uremic syndrome after shigellosis. Relation to endotoxemia and circulating immune complexes*. The New England journal of medicine, 1978. **298**(17): p. 927-33.
19. Navaneethan, U. and R.A. Giannella, *Infectious colitis*. Current opinion in gastroenterology, 2011. **27**(1): p. 66-71.

20. Lim, J.Y., J. Yoon, and C.J. Hovde, *A brief overview of Escherichia coli O157:H7 and its plasmid O157*. Journal of microbiology and biotechnology, 2010. **20**(1): p. 5-14.
21. Melton-Celsa, A., et al., *Pathogenesis of Shiga-toxin producing escherichia coli*. Current topics in microbiology and immunology, 2012. **357**: p. 67-103.
22. Wong, C.S., et al., *The risk of the hemolytic-uremic syndrome after antibiotic treatment of Escherichia coli O157:H7 infections*. The New England journal of medicine, 2000. **342**(26): p. 1930-6.
23. Goode, B., et al., *Outbreak of escherichia coli O157: H7 infections after Petting Zoo visits, North Carolina State Fair, October-November 2004*. Archives of pediatrics & adolescent medicine, 2009. **163**(1): p. 42-8.
24. Scheiring, J., S.P. Andreoli, and L.B. Zimmerhackl, *Treatment and outcome of Shiga-toxin-associated hemolytic uremic syndrome (HUS)*. Pediatric nephrology, 2008. **23**(10): p. 1749-60.
25. Psotka, M.A., et al., *Shiga toxin 2 targets the murine renal collecting duct epithelium*. Infection and immunity, 2009. **77**(3): p. 959-69.
26. Sherman, P.M., J.C. Ossa, and E. Wine, *Bacterial infections: new and emerging enteric pathogens*. Current opinion in gastroenterology, 2010. **26**(1): p. 1-4.
27. Noris, M. and G. Remuzzi, *Atypical hemolytic-uremic syndrome*. The New England journal of medicine, 2009. **361**(17): p. 1676-87.
28. Eriksson, K.J., S.G. Boyd, and R.C. Tasker, *Acute neurology and neurophysiology of haemolytic-uraemic syndrome*. Archives of disease in childhood, 2001. **84**(5): p. 434-5.
29. Goldwater, P.N. and K.A. Bettelheim, *Treatment of enterohemorrhagic Escherichia coli (EHEC) infection and hemolytic uremic syndrome (HUS)*. BMC medicine, 2012. **10**: p. 12.
30. Tenailon, O., et al., *The population genetics of commensal Escherichia coli*. Nature reviews. Microbiology, 2010. **8**(3): p. 207-17.
31. Farfan, M.J. and A.G. Torres, *Molecular mechanisms that mediate colonization of Shiga toxin-producing Escherichia coli strains*. Infection and immunity, 2012. **80**(3): p. 903-13.
32. Wick, L.M., et al., *Evolution of genomic content in the stepwise emergence of Escherichia coli O157:H7*. Journal of bacteriology, 2005. **187**(5): p. 1783-91.
33. Chinen, I., et al., *Shiga toxin-producing Escherichia coli O157 in beef and chicken burgers, and chicken carcasses in Buenos Aires, Argentina*. International journal of food microbiology, 2009. **132**(2-3): p. 167-71.
34. Pawlowski, S.W., C.A. Warren, and R. Guerrant, *Diagnosis and treatment of acute or persistent diarrhea*. Gastroenterology, 2009. **136**(6): p. 1874-86.
35. Kodama, T., *[Mechanism of A/E lesion formation produced by enterohemorrhagic Escherichia coli: O157--role of EspB, Tir and cortactin]*. Nihon rinsho. Japanese journal of clinical medicine, 2002. **60**(6): p. 1101-7.
36. Schmidt, M.A., *LEEWays: tales of EPEC, ATEC and EHEC*. Cellular microbiology, 2010. **12**(11): p. 1544-52.
37. Kaper, J.B., J.P. Nataro, and H.L. Mobley, *Pathogenic Escherichia coli*. Nature reviews. Microbiology, 2004. **2**(2): p. 123-40.

38. FDA, *Bad Bug Book: Handbook of Foodborne Pathogenic Microorganisms and Natural Toxins*, FDA, Editor 2012, FDA. p. 264.
39. Nataro, J.P. and J.B. Kaper, *Diarrheagenic Escherichia coli*. *Clinical microbiology reviews*, 1998. **11**(1): p. 142-201.
40. Omisakin, F., et al., *Concentration and prevalence of Escherichia coli O157 in cattle feces at slaughter*. *Applied and environmental microbiology*, 2003. **69**(5): p. 2444-7.
41. Chase-Topping, M.E., et al., *Risk factors for the presence of high-level shedders of Escherichia coli O157 on Scottish farms*. *Journal of clinical microbiology*, 2007. **45**(5): p. 1594-603.
42. Tobe, T., et al., *Complete DNA sequence and structural analysis of the enteropathogenic Escherichia coli adherence factor plasmid*. *Infect Immun*, 1999. **67**(10): p. 5455-62.
43. Mundy, R., et al., *Citrobacter rodentium of mice and man*. *Cellular microbiology*, 2005. **7**(12): p. 1697-706.
44. Wiles, S., et al., *Organ specificity, colonization and clearance dynamics in vivo following oral challenges with the murine pathogen Citrobacter rodentium*. *Cellular microbiology*, 2004. **6**(10): p. 963-72.
45. Barthold, S.W., et al., *Transmissible murine colonic hyperplasia*. *Veterinary pathology*, 1978. **15**(2): p. 223-36.
46. Schauer, D.B., et al., *Genetic and biochemical characterization of Citrobacter rodentium sp. nov.* *Journal of clinical microbiology*, 1995. **33**(8): p. 2064-8.
47. Deng, W., et al., *Locus of enterocyte effacement from Citrobacter rodentium: sequence analysis and evidence for horizontal transfer among attaching and effacing pathogens*. *Infection and immunity*, 2001. **69**(10): p. 6323-35.
48. Wales, A.D., M.J. Woodward, and G.R. Pearson, *Attaching-effacing bacteria in animals*. *Journal of comparative pathology*, 2005. **132**(1): p. 1-26.
49. Schauer, D.B. and S. Falkow, *The eae gene of Citrobacter freundii biotype 4280 is necessary for colonization in transmissible murine colonic hyperplasia*. *Infect Immun*, 1993. **61**(11): p. 4654-61.
50. Schauer, D.B. and S. Falkow, *Attaching and effacing locus of a Citrobacter freundii biotype that causes transmissible murine colonic hyperplasia*. *Infect Immun*, 1993. **61**(6): p. 2486-92.
51. Garmendia, J., G. Frankel, and V.F. Crepin, *Enteropathogenic and enterohemorrhagic Escherichia coli infections: translocation, translocation, translocation*. *Infection and immunity*, 2005. **73**(5): p. 2573-85.
52. Krogfelt, K.A., *Bacterial adhesion: genetics, biogenesis, and role in pathogenesis of fimbrial adhesins of Escherichia coli*. *Reviews of infectious diseases*, 1991. **13**(4): p. 721-35.
53. Stone, K.D., et al., *A cluster of fourteen genes from enteropathogenic Escherichia coli is sufficient for the biogenesis of a type IV pilus*. *Molecular microbiology*, 1996. **20**(2): p. 325-37.
54. Hicks, S., et al., *Role of intimin and bundle-forming pili in enteropathogenic Escherichia coli adhesion to pediatric intestinal tissue in vitro*. *Infection and immunity*, 1998. **66**(4): p. 1570-8.

55. Bieber, D., et al., *Type IV pili, transient bacterial aggregates, and virulence of enteropathogenic Escherichia coli*. Science, 1998. **280**(5372): p. 2114-8.
56. Giron, J.A., A.S. Ho, and G.K. Schoolnik, *An inducible bundle-forming pilus of enteropathogenic Escherichia coli*. Science, 1991. **254**(5032): p. 710-3.
57. Winardhi, R.S., et al., *Higher order oligomerization is required for H-NS family member MvaT to form gene-silencing nucleoprotein filament*. Nucleic acids research, 2012. **40**(18): p. 8942-8952.
58. Elliott, S.J., et al., *The complete sequence of the locus of enterocyte effacement (LEE) from enteropathogenic Escherichia coli E2348/69*. Molecular microbiology, 1998. **28**(1): p. 1-4.
59. Bardiau, M., M. Szalo, and J.G. Mainil, *Initial adherence of EPEC, EHEC and VTEC to host cells*. Veterinary research, 2010. **41**(5): p. 57.
60. Baumler, A.J., R.M. Tsolis, and F. Heffron, *The Ipf fimbrial operon mediates adhesion of Salmonella typhimurium to murine Peyer's patches*. Proceedings of the National Academy of Sciences of the United States of America, 1996. **93**(1): p. 279-83.
61. Rosqvist, R., K.E. Magnusson, and H. Wolf-Watz, *Target cell contact triggers expression and polarized transfer of Yersinia YopE cytotoxin into mammalian cells*. The EMBO journal, 1994. **13**(4): p. 964-72.
62. Erhardt, M., K. Namba, and K.T. Hughes, *Bacterial nanomachines: the flagellum and type III injectisome*. Cold Spring Harbor perspectives in biology, 2010. **2**(11): p. a000299.
63. Frankel, G., et al., *Enteropathogenic and enterohaemorrhagic Escherichia coli: more subversive elements*. Molecular microbiology, 1998. **30**(5): p. 911-21.
64. Knutton, S., et al., *A novel EspA-associated surface organelle of enteropathogenic Escherichia coli involved in protein translocation into epithelial cells*. The EMBO journal, 1998. **17**(8): p. 2166-76.
65. Kimbrough, T.G. and S.I. Miller, *Assembly of the type III secretion needle complex of Salmonella typhimurium*. Microbes and infection / Institut Pasteur, 2002. **4**(1): p. 75-82.
66. Kenny, B. and B.B. Finlay, *Protein secretion by enteropathogenic Escherichia coli is essential for transducing signals to epithelial cells*. Proceedings of the National Academy of Sciences of the United States of America, 1995. **92**(17): p. 7991-5.
67. Kenny, B., et al., *Enteropathogenic E. coli (EPEC) transfers its receptor for intimate adherence into mammalian cells*. Cell, 1997. **91**(4): p. 511-20.
68. Daniell, S.J., et al., *The filamentous type III secretion translocon of enteropathogenic Escherichia coli*. Cellular microbiology, 2001. **3**(12): p. 865-71.
69. Sekiya, K., et al., *Supermolecular structure of the enteropathogenic Escherichia coli type III secretion system and its direct interaction with the EspA-sheath-like structure*. Proceedings of the National Academy of Sciences of the United States of America, 2001. **98**(20): p. 11638-43.
70. Abe, A., et al., *Two enteropathogenic Escherichia coli type III secreted proteins, EspA and EspB, are virulence factors*. The Journal of experimental medicine, 1998. **188**(10): p. 1907-16.

71. Lai, L.C., et al., *A third secreted protein that is encoded by the enteropathogenic Escherichia coli pathogenicity island is required for transduction of signals and for attaching and effacing activities in host cells*. Infection and immunity, 1997. **65**(6): p. 2211-7.
72. Taylor, K.A., et al., *The EspB protein of enteropathogenic Escherichia coli is targeted to the cytoplasm of infected HeLa cells*. Infection and immunity, 1998. **66**(11): p. 5501-7.
73. McDaniel, T.K., *Ph.D. thesis*, 1996, University of Maryland: Baltimore.
74. Mellies, J.L., et al., *The Per regulon of enteropathogenic Escherichia coli : identification of a regulatory cascade and a novel transcriptional activator, the locus of enterocyte effacement (LEE)-encoded regulator (Ler)*. Molecular microbiology, 1999. **33**(2): p. 296-306.
75. Elliott, S.J., et al., *The locus of enterocyte effacement (LEE)-encoded regulator controls expression of both LEE- and non-LEE-encoded virulence factors in enteropathogenic and enterohemorrhagic Escherichia coli*. Infection and immunity, 2000. **68**(11): p. 6115-26.
76. Sperandio, V., et al., *Activation of enteropathogenic Escherichia coli (EPEC) LEE2 and LEE3 operons by Ler*. Molecular microbiology, 2000. **38**(4): p. 781-93.
77. Sperandio, V., et al., *Quorum sensing controls expression of the type III secretion gene transcription and protein secretion in enterohemorrhagic and enteropathogenic Escherichia coli*. Proceedings of the National Academy of Sciences of the United States of America, 1999. **96**(26): p. 15196-201.
78. Torres, A.G., et al., *Ler and H-NS, regulators controlling expression of the long polar fimbriae of Escherichia coli O157:H7*. Journal of bacteriology, 2007. **189**(16): p. 5916-28.
79. Bustamante, V.H., et al., *Transcriptional regulation of type III secretion genes in enteropathogenic Escherichia coli: Ler antagonizes H-NS-dependent repression*. Molecular microbiology, 2001. **39**(3): p. 664-78.
80. Barba, J., et al., *A positive regulatory loop controls expression of the locus of enterocyte effacement-encoded regulators Ler and GrlA*. Journal of bacteriology, 2005. **187**(23): p. 7918-30.
81. Iyoda, S. and H. Watanabe, *ClpXP protease controls expression of the type III protein secretion system through regulation of RpoS and GrlR levels in enterohemorrhagic Escherichia coli*. Journal of bacteriology, 2005. **187**(12): p. 4086-94.
82. Creasey, E.A., et al., *Yeast two-hybrid system survey of interactions between LEE-encoded proteins of enteropathogenic Escherichia coli*. Microbiology, 2003. **149**(Pt 8): p. 2093-106.
83. Lio, J.C. and W.J. Syu, *Identification of a negative regulator for the pathogenicity island of enterohemorrhagic Escherichia coli O157:H7*. Journal of biomedical science, 2004. **11**(6): p. 855-63.
84. Brunder, W., et al., *The large plasmids of Shiga-toxin-producing Escherichia coli (STEC) are highly variable genetic elements*. Microbiology, 1999. **145** (Pt 5): p. 1005-14.

85. Schmidt, H., L. Beutin, and H. Karch, *Molecular analysis of the plasmid-encoded hemolysin of Escherichia coli O157:H7 strain EDL 933*. Infection and immunity, 1995. **63**(3): p. 1055-61.
86. Welch, R.A., *Pore-forming cytolysins of gram-negative bacteria*. Molecular microbiology, 1991. **5**(3): p. 521-8.
87. Law, D. and J. Kelly, *Use of heme and hemoglobin by Escherichia coli O157 and other Shiga-like-toxin-producing E. coli serogroups*. Infection and immunity, 1995. **63**(2): p. 700-2.
88. Karpman, D., L. Sartz, and S. Johnson, *Pathophysiology of typical hemolytic uremic syndrome*. Seminars in thrombosis and hemostasis, 2010. **36**(6): p. 575-85.
89. Zoja, C., et al., *Verotoxin glycolipid receptors determine the localization of microangiopathic process in rabbits given verotoxin-1*. The Journal of laboratory and clinical medicine, 1992. **120**(2): p. 229-38.
90. Obata, F., et al., *Shiga toxin 2 affects the central nervous system through receptor globotriaosylceramide localized to neurons*. The Journal of Infectious Diseases, 2008. **198**(9): p. 1398-406.
91. Tironi-Farinati, C., et al., *Intracerebroventricular Shiga toxin 2 increases the expression of its receptor globotriaosylceramide and causes dendritic abnormalities*. Journal of neuroimmunology, 2010. **222**(1-2): p. 48-61.
92. Lukyanenko, V., et al., *Enterohemorrhagic Escherichia coli infection stimulates Shiga toxin 1 macropinocytosis and transcytosis across intestinal epithelial cells*. American journal of physiology. Cell physiology, 2011. **301**(5): p. C1140-9.
93. Obrig, T.G., T.P. Moran, and J.E. Brown, *The mode of action of Shiga toxin on peptide elongation of eukaryotic protein synthesis*. The Biochemical journal, 1987. **244**(2): p. 287-94.
94. Sandvig, K., et al., *Endocytosis and retrograde transport of Shiga toxin*. Toxicon : official journal of the International Society on Toxinology, 2010. **56**(7): p. 1181-5.
95. Sandvig, K. and B. van Deurs, *Entry of ricin and Shiga toxin into cells: molecular mechanisms and medical perspectives*. The EMBO journal, 2000. **19**(22): p. 5943-50.
96. Asakura, H., et al., *Phylogenetic diversity and similarity of active sites of Shiga toxin (stx) in Shiga toxin-producing Escherichia coli (STEC) isolates from humans and animals*. Epidemiology and infection, 2001. **127**(1): p. 27-36.
97. Coombes, B.K., et al., *Molecular analysis as an aid to assess the public health risk of non-O157 Shiga toxin-producing Escherichia coli strains*. Applied and environmental microbiology, 2008. **74**(7): p. 2153-60.
98. Echtenkamp, F., et al., *Characterization of the NleF effector protein from attaching and effacing bacterial pathogens*. FEMS microbiology letters, 2008. **281**(1): p. 98-107.
99. Tobe, T., et al., *An extensive repertoire of type III secretion effectors in Escherichia coli O157 and the role of lambdoid phages in their dissemination*. Proc Natl Acad Sci U S A, 2006. **103**(40): p. 14941-6.
100. Kim, J., et al., *The bacterial virulence factor NleA inhibits cellular protein secretion by disrupting mammalian COPII function*. Cell host & microbe, 2007. **2**(3): p. 160-71.

101. Kuhle, V., G.L. Abrahams, and M. Hensel, *Intracellular Salmonella enterica redirect exocytic transport processes in a Salmonella pathogenicity island 2-dependent manner*. Traffic, 2006. **7**(6): p. 716-30.
102. Robinson, C.G. and C.R. Roy, *Attachment and fusion of endoplasmic reticulum with vacuoles containing Legionella pneumophila*. Cellular microbiology, 2006. **8**(5): p. 793-805.
103. Steele-Mortimer, O., et al., *Biogenesis of Salmonella typhimurium-containing vacuoles in epithelial cells involves interactions with the early endocytic pathway*. Cellular microbiology, 1999. **1**(1): p. 33-49.
104. Cuellar-Mata, P., et al., *Nramp1 modifies the fusion of Salmonella typhimurium-containing vacuoles with cellular endomembranes in macrophages*. The Journal of biological chemistry, 2002. **277**(3): p. 2258-65.
105. Celli, J., S.P. Salcedo, and J.P. Gorvel, *Brucella coopts the small GTPase Sar1 for intracellular replication*. Proceedings of the National Academy of Sciences of the United States of America, 2005. **102**(5): p. 1673-8.
106. Alberts, B., *Molecular biology of the cell*. 4th ed2002, New York: Garland Science. xxxiv, 1548 p.
107. Lodish, H.F., *Molecular cell biology*. 6th ed2008, New York: W.H. Freeman.
108. Gilmore, R., G. Blobel, and P. Walter, *Protein translocation across the endoplasmic reticulum. I. Detection in the microsomal membrane of a receptor for the signal recognition particle*. The Journal of cell biology, 1982. **95**(2 Pt 1): p. 463-9.
109. Walter, P. and G. Blobel, *Subcellular distribution of signal recognition particle and 7SL-RNA determined with polypeptide-specific antibodies and complementary DNA probe*. The Journal of cell biology, 1983. **97**(6): p. 1693-9.
110. Strating, J.R., T.G. Hafmans, and G.J. Martens, *COP-binding sites in p24delta2 are necessary for proper secretory cargo biosynthesis*. The international journal of biochemistry & cell biology, 2009. **41**(7): p. 1619-27.
111. Strating, J.R., T.G. Hafmans, and G.J. Martens, *Functional diversity among p24 subfamily members*. Biology of the cell / under the auspices of the European Cell Biology Organization, 2009. **101**(4): p. 207-19.
112. Strating, J.R. and G.J. Martens, *The p24 family and selective transport processes at the ER-Golgi interface*. Biology of the cell / under the auspices of the European Cell Biology Organization, 2009. **101**(9): p. 495-509.
113. Strating, J.R., et al., *A comprehensive overview of the vertebrate p24 family: identification of a novel tissue-specifically expressed member*. Molecular biology and evolution, 2009. **26**(8): p. 1707-14.
114. Braakman, I. and N.J. Balleid, *Protein folding and modification in the mammalian endoplasmic reticulum*. Annual review of biochemistry, 2011. **80**: p. 71-99.
115. Barlowe, C., et al., *COPII: a membrane coat formed by Sec proteins that drive vesicle budding from the endoplasmic reticulum*. Cell, 1994. **77**(6): p. 895-907.
116. Aridor, M., et al., *Sequential coupling between COPII and COPI vesicle coats in endoplasmic reticulum to Golgi transport*. The Journal of cell biology, 1995. **131**(4): p. 875-93.

117. Scales, S.J., R. Pepperkok, and T.E. Kreis, *Visualization of ER-to-Golgi transport in living cells reveals a sequential mode of action for COPII and COPI*. Cell, 1997. **90**(6): p. 1137-48.
118. Mogelsvang, S. and K.E. Howell, *Global approaches to study Golgi function*. Current opinion in cell biology, 2006. **18**(4): p. 438-43.
119. Bonfanti, L., et al., *Procollagen traverses the Golgi stack without leaving the lumen of cisternae: evidence for cisternal maturation*. Cell, 1998. **95**(7): p. 993-1003.
120. Losev, E., et al., *Golgi maturation visualized in living yeast*. Nature, 2006. **441**(7096): p. 1002-6.
121. Glick, B.S. and V. Malhotra, *The curious status of the Golgi apparatus*. Cell, 1998. **95**(7): p. 883-9.
122. Matsuura-Tokita, K., et al., *Live imaging of yeast Golgi cisternal maturation*. Nature, 2006. **441**(7096): p. 1007-10.
123. Dominguez, M., et al., *gp25L/emp24/p24 protein family members of the cis-Golgi network bind both COP I and II coatomer*. The Journal of cell biology, 1998. **140**(4): p. 751-65.
124. Anantharaman, V. and L. Aravind, *The GOLD domain, a novel protein module involved in Golgi function and secretion*. Genome biology, 2002. **3**(5): p. research0023.
125. Emery, G., J. Gruenberg, and M. Rojo, *The p24 family of transmembrane proteins at the interface between endoplasmic reticulum and Golgi apparatus*. Protoplasma, 1999(207): p. 24-30.
126. Stamnes, M.A., et al., *An integral membrane component of coatomer-coated transport vesicles defines a family of proteins involved in budding*. Proceedings of the National Academy of Sciences of the United States of America, 1995. **92**(17): p. 8011-5.
127. Marelli, M., et al., *Quantitative mass spectrometry reveals a role for the GTPase Rho1p in actin organization on the peroxisome membrane*. The Journal of cell biology, 2004. **167**(6): p. 1099-112.
128. Hosaka, M., et al., *A subset of p23 localized on secretory granules in pancreatic beta-cells*. The journal of histochemistry and cytochemistry : official journal of the Histochemistry Society, 2007. **55**(3): p. 235-45.
129. Bethune, J., F. Wieland, and J. Moelleken, *COPI-mediated transport*. The Journal of membrane biology, 2006. **211**(2): p. 65-79.
130. Schiulki, I. and A. Volchuk, *Diverse roles for the p24 family of proteins in eukaryotic cells*. Biomolecular Concepts, 2012. **0**(0): p. 1-10.
131. Jenne, N., et al., *Oligomeric state and stoichiometry of p24 proteins in the early secretory pathway*. The Journal of biological chemistry, 2002. **277**(48): p. 46504-11.
132. Ciuffo, L.F. and A. Boyd, *Identification of a luminal sequence specifying the assembly of Emp24p into p24 complexes in the yeast secretory pathway*. The Journal of biological chemistry, 2000. **275**(12): p. 8382-8.
133. Wada, I., et al., *SSR alpha and associated calnexin are major calcium binding proteins of the endoplasmic reticulum membrane*. The Journal of biological chemistry, 1991. **266**(29): p. 19599-610.

134. Belden, W.J. and C. Barlowe, *Erv25p, a component of COPII-coated vesicles, forms a complex with Emp24p that is required for efficient endoplasmic reticulum to Golgi transport*. The Journal of biological chemistry, 1996. **271**(43): p. 26939-46.
135. Blum, R., et al., *Tmp21 and p24A, two type I proteins enriched in pancreatic microsomal membranes, are members of a protein family involved in vesicular trafficking*. J Biol Chem, 1996. **271**(29): p. 17183-9.
136. Sohn, K., et al., *A major transmembrane protein of Golgi-derived COPI-coated vesicles involved in coatamer binding*. The Journal of cell biology, 1996. **135**(5): p. 1239-48.
137. Nickel, W., et al., *p23, a major COPI-vesicle membrane protein, constitutively cycles through the early secretory pathway*. Proceedings of the National Academy of Sciences of the United States of America, 1997. **94**(21): p. 11393-8.
138. Blum, R., et al., *Intracellular localization and in vivo trafficking of p24A and p23*. Journal of cell science, 1999. **112 (Pt 4)**: p. 537-48.
139. Gommel, D., et al., *p24 and p23, the major transmembrane proteins of COPI-coated transport vesicles, form hetero-oligomeric complexes and cycle between the organelles of the early secretory pathway*. FEBS letters, 1999. **447**(2-3): p. 179-85.
140. Fullekrug, J., et al., *Localization and recycling of gp27 (hp24gamma3): complex formation with other p24 family members*. Molecular biology of the cell, 1999. **10**(6): p. 1939-55.
141. Emery, G., M. Rojo, and J. Gruenberg, *Coupled transport of p24 family members*. Journal of cell science, 2000. **113 (Pt 13)**: p. 2507-16.
142. Langhans, M., et al., *In vivo trafficking and localization of p24 proteins in plant cells*. Traffic, 2008. **9**(5): p. 770-85.
143. Gommel, D.U., et al., *Recruitment to Golgi membranes of ADP-ribosylation factor 1 is mediated by the cytoplasmic domain of p23*. The EMBO journal, 2001. **20**(23): p. 6751-60.
144. Wessels, E., et al., *A viral protein that blocks Arf1-mediated COP-I assembly by inhibiting the guanine nucleotide exchange factor GBF1*. Developmental cell, 2006. **11**(2): p. 191-201.
145. Harter, C. and F.T. Wieland, *A single binding site for dilysine retrieval motifs and p23 within the gamma subunit of coatamer*. Proceedings of the National Academy of Sciences of the United States of America, 1998. **95**(20): p. 11649-54.
146. Cosson, P. and F. Letourneur, *Coatamer interaction with di-lysine endoplasmic reticulum retention motifs*. Science, 1994. **263**(5153): p. 1629-31.
147. Jackson, M.R., T. Nilsson, and P.A. Peterson, *Identification of a consensus motif for retention of transmembrane proteins in the endoplasmic reticulum*. The EMBO journal, 1990. **9**(10): p. 3153-62.
148. Letourneur, F., et al., *Coatamer is essential for retrieval of dilysine-tagged proteins to the endoplasmic reticulum*. Cell, 1994. **79**(7): p. 1199-207.
149. Bremser, M., et al., *Coupling of coat assembly and vesicle budding to packaging of putative cargo receptors*. Cell, 1999. **96**(4): p. 495-506.

150. Reinhard, C., et al., *Receptor-induced polymerization of coatomer*. Proceedings of the National Academy of Sciences of the United States of America, 1999. **96**(4): p. 1224-8.
151. Nickel, W. and F.T. Wieland, *Receptor-dependent formation of COPI-coated vesicles from chemically defined donor liposomes*. Methods in enzymology, 2001. **329**: p. 388-404.
152. Zhao, L., et al., *GTP-dependent binding of ADP-ribosylation factor to coatomer in close proximity to the binding site for dilysine retrieval motifs and p23*. The Journal of biological chemistry, 1999. **274**(20): p. 14198-203.
153. Schimmoller, F., et al., *The absence of Emp24p, a component of ER-derived COPII-coated vesicles, causes a defect in transport of selected proteins to the Golgi*. The EMBO journal, 1995. **14**(7): p. 1329-39.
154. Denzel, A., et al., *The p24 family member p23 is required for early embryonic development*. Current biology : CB, 2000. **10**(1): p. 55-8.
155. Elrod-Erickson, M.J. and C.A. Kaiser, *Genes that control the fidelity of endoplasmic reticulum to Golgi transport identified as suppressors of vesicle budding mutations*. Molecular biology of the cell, 1996. **7**(7): p. 1043-58.
156. Kaiser, C. and S. Ferro-Novick, *Transport from the endoplasmic reticulum to the Golgi*. Current opinion in cell biology, 1998. **10**(4): p. 477-82.
157. Baba, T., et al., *Role of dynamin in clathrin-coated vesicle formation*. Cold Spring Harb Symp Quant Biol, 1995. **60**: p. 235-42.
158. Barlowe, C., *Coupled ER to Golgi transport reconstituted with purified cytosolic proteins*. J Cell Biol, 1997. **139**(5): p. 1097-108.
159. Blumental-Perry, A., et al., *Phosphatidylinositol 4-phosphate formation at ER exit sites regulates ER export*. Developmental cell, 2006. **11**(5): p. 671-82.
160. Derby, M.C., et al., *Mammalian GRIP domain proteins differ in their membrane binding properties and are recruited to distinct domains of the TGN*. Journal of cell science, 2004. **117**(Pt 24): p. 5865-74.
161. Diao, A., et al., *Coordination of golgin tethering and SNARE assembly: GM130 binds syntaxin 5 in a p115-regulated manner*. J Biol Chem, 2008. **283**(11): p. 6957-67.
162. Chen, F., et al., *TMP21 is a presenilin complex component that modulates gamma-secretase but not epsilon-secretase activity*. Nature, 2006. **440**(7088): p. 1208-12.
163. Wang, H., L. Xiao, and M.G. Kazanietz, *p23/Tmp21 associates with protein kinase Cdelta (PKCdelta) and modulates its apoptotic function*. The Journal of biological chemistry, 2011. **286**(18): p. 15821-31.
164. Presley, J.F., et al., *ER-to-Golgi transport visualized in living cells*. Nature, 1997. **389**(6646): p. 81-5.
165. Aguilera-Romero, A., et al., *The yeast p24 complex is required for the formation of COPI retrograde transport vesicles from the Golgi apparatus*. The Journal of cell biology, 2008. **180**(4): p. 713-20.
166. Anantharaman, V. and L. Aravind, *The GOLD domain, a novel protein module involved in Golgi function and secretion*. Genome Biol, 2002. **3**(5): p. research0023.

167. Gommel, D.U., et al., *Recruitment to Golgi membranes of ADP-ribosylation factor 1 is mediated by the cytoplasmic domain of p23*. *Embo J*, 2001. **20**(23): p. 6751-60.
168. Aguilera-Romero, A., et al., *The yeast p24 complex is required for the formation of COPI retrograde transport vesicles from the Golgi apparatus*. *J Cell Biol*, 2008. **180**(4): p. 713-20.
169. Echtenkamp, F., et al., *Characterization of the NleF effector protein from attaching and effacing bacterial pathogens*. *FEMS Microbiol Lett*, 2008. **281**(1): p. 98-107.
170. Blum, R. and A. Lepier, *The luminal domain of p23 (Tnp21) plays a critical role in p23 cell surface trafficking*. *Traffic*, 2008. **9**(9): p. 1530-50.
171. Wessels, E., et al., *A proline-rich region in the coxsackievirus 3A protein is required for the protein to inhibit endoplasmic reticulum-to-golgi transport*. *J Virol*, 2005. **79**(8): p. 5163-73.
172. Lippincott-Schwartz, J., T.H. Roberts, and K. Hirschberg, *Secretory protein trafficking and organelle dynamics in living cells*. *Annu Rev Cell Dev Biol*, 2000. **16**: p. 557-89.